Studies of jet mass in dijet and W/Z + jet events

CMS Collaboration ; Chatrchyan, S ; Khachatryan, V ; Sirunyan, A M ; et al ; Chiochia, V ; Kilminster, B ; Robmann, P

Abstract: Invariant mass spectra for jets reconstructed using the anti-k T and CambridgeAachen algorithms are studied for different jet "grooming" techniques in data corresponding to an integrated luminosity of 5 fb−1, recorded with the CMS detector in proton-proton collisions at the LHC at a center-of-mass energy of 7 TeV. Leading-order QCD predictions for inclusive dijet and W/Z+jet production combined with parton-shower Monte Carlo models are found to agree overall with the data, and the agreement improves with the implementation of jet grooming methods used to distinguish merged jets of large transverse momentum from softer QCD gluon radiation.

DOI: https://doi.org/10.1007/JHEP05(2013)090

Published for SISSA by Springer

Received: *March 20, 2013*
Accepted: *April 30, 2013*
Published: *May 17, 2013*

Studies of jet mass in dijet and W/Z + jet events

The CMS collaboration

E-mail: cms-publication-committee-chair@cern.ch

Abstract: Invariant mass spectra for jets reconstructed using the anti-k_T and Cambridge-Aachen algorithms are studied for different jet "grooming" techniques in data corresponding to an integrated luminosity of $5\,\text{fb}^{-1}$, recorded with the CMS detector in proton-proton collisions at the LHC at a center-of-mass energy of 7 TeV. Leading-order QCD predictions for inclusive dijet and W/Z+jet production combined with parton-shower Monte Carlo models are found to agree overall with the data, and the agreement improves with the implementation of jet grooming methods used to distinguish merged jets of large transverse momentum from softer QCD gluon radiation.

Keywords: Hadron-Hadron Scattering

doi:10.1007/JHEP05(2013)090

JHEP05(2013)090

Contents

1 Introduction

The variables most often used in analyses of jet production are jet directions and transverse momenta (p_{T}). However, as jets are composite objects, their invariant masses (m_J) provide additional information that can be used to characterize their properties. One motivation for investigating jet mass is that, at the Large Hadron Collider (LHC), massive standard model (SM) particles such as W and Z bosons and top quarks are often produced with large Lorentz boosts, and, when such particles decay into quarks, the masses of the

JHEP05(2013)090

evolved jets can be used to discriminate them from lighter objects generated in quantum-chromodynamic (QCD) radiative processes. The same argument also holds for any new massive particles produced at the LHC. For sufficiently large boosts, all the decay products tend to be emitted as collimated groupings into small sections of the detector, and the resulting particles can be clustered into a single jet. Jet "grooming" techniques are designed to separate such merged jets from background. These new techniques have been found to be very promising for identifying decays of highly-boosted W bosons and top quarks, and in searches for Higgs bosons and other massive particles [1]. The main advantage of these grooming techniques is their ability to distinguish high p_{T} jets that arise from decays of massive, possibly new, particles. In addition, their robust performance is valuable in the presence of additional interactions in an event (pileup), which is likely to provide an even greater challenge to such analyses in future higher-luminosity runs at the LHC.

Only a few of these promising approaches have been studied in data at the Tevatron [2] or at the LHC [3]. To understand these techniques in the context of searches for new phenomena, the jet mass must be well-modeled through leading-order (LO) or next-to-leading-order (NLO) Monte Carlo (MC) simulations. Much recent theoretical work in QCD has focused on the computation of jet mass, including predictions using advances in an effective field theory of jets (soft collinear effective theory, SCET) [4–23]. Studies of the kind reported in the present analysis can provide an understanding of the extent to which MC simulations that match matrix-element partons with parton showers can model the observed internal jet structure. Results of these studies can also be used to compare data with theoretical computations of jet mass, and to provide benchmarks for the use of these algorithms in searches for highly-boosted Higgs bosons, or new objects beyond the SM, especially by investigating some of the background processes expected in such analyses.

We present a measurement of jet mass in a sample of dijet events, and the first study of such distributions in V+jet events, where V refers to a W or Z boson. The data correspond to an integrated luminosity of $5.0 \pm 0.2\,\mathrm{fb}^{-1}$, collected by the Compact Muon Solenoid (CMS) experiment at the LHC in pp interactions at a center-of-mass energy of 7 TeV. The analysis of these two types of final states provides complementary information because of their different parton-flavor content, since the selected dijet events are dominated by gluon-initiated jets, and the V+jet events often contain quark-initiated jets. We focus on measuring the jet mass after applying several jet grooming techniques involving "filtering" [24], "trimming" [25], and "pruning" [26, 27] of jets, as discussed in detail below. This work also presents the first attempt to measure the mass of trimmed and pruned jets.

To study the dependence of the differential distributions in m_J on jet p_{T}, we measure the distributions in intervals of jet transverse momentum. Formally, this can be expressed in terms of a double-differential cross section for jet production ($d^2\sigma/dp_{\mathrm{T}}dm_J$) that is examined as a function of m_J for several nonoverlapping intervals in p_{T}:

$$\sigma = \int_{m_J}\int_{p_{\mathrm{T}}} \frac{\mathrm{d}^2\sigma(m_J, p_{\mathrm{T}})}{\mathrm{d}m_J\,\mathrm{d}p_{\mathrm{T}}}\,\mathrm{d}p_{\mathrm{T}}\,\mathrm{d}m_J = \sum_i \int_{m_J} \frac{\mathrm{d}\sigma_i(m_J)}{\mathrm{d}m_J}\,\mathrm{d}m_J = \sum_i \sigma_i, \tag{1.1}$$

where $i = 1, 2, 3, \ldots$ refers to the i^{th} interval in p_{T}, and the sum of contributions over all i is equal to the total observed cross section $\sum_i \sigma_i = \sigma$. The differential probability density

JHEP05(2013)090

as a function of m_J for each p_T interval can therefore be written as

$$\rho_i(m_J) = \frac{1}{\sigma_i} \times \frac{\mathrm{d}\sigma_i}{\mathrm{d}m_J}, \text{ with } \int \rho_i(m_J)\,\mathrm{d}m_J = 1. \tag{1.2}$$

The distributions in reconstructed jet mass of eq. (1.2) include corrections used to unfold jets to the "particle" level; the p_T intervals are defined for ungroomed jets, following energy corrections for the response of the detector.

For the dijet analysis, p_T and m_J correspond to the average transverse momentum and average jet mass of the two leading jets (i.e., of highest p_T): $p_T^{AVG} = (p_{T1} + p_{T2})/2$ and $m_J^{AVG} = (m_{J1} + m_{J2})/2$. For the V+jet analysis, we use the m_J and p_T of the leading jet. Both quantities depend on the nature of the jet grooming algorithm, as discussed in section 2.

This paper is organized as follows. To introduce the subject, we first discuss jet clustering algorithms in section 2, focusing mainly on grooming techniques. After a brief description of the CMS detector and the MC samples in section 3, we provide information pertaining to the collected data and a description of event reconstruction in section 4. Selection of events is then described in section 5, and the effect of pileup on jet mass is investigated in section 6. This is followed in section 7 by the correction and unfolding procedures that are applied to the m_J spectra and their corresponding systematic uncertainties. In sections 8 and 9, we present the results of the dijet and V+jet analyses, respectively. Finally, observations and remarks on the presented results are summarized in section 10.

The distributions shown are also stored in HEPData format [28].

2 Jet clustering algorithms and grooming techniques

2.1 Sequential jet clustering algorithms

Jets are defined through sequential, iterative jet clustering algorithms that combine four-vectors of input pairs of particles until certain criteria are satisfied and jets are formed. For the jet algorithms considered in this paper, for each pair of particles i and j, a "distance" metric between the two particles (d_{ij}), and the so-called "beam distance" for each particle (d_{iB}), are computed:

$$d_{ij} = \min({p_T}_i^{2n}, {p_T}_j^{2n})\Delta R_{ij}^2/R^2 \tag{2.1}$$

$$d_{iB} = {p_T}_i^{2n}, \tag{2.2}$$

where p_{Ti} and p_{Tj} are the transverse momenta of particles i and j, respectively, "min" refers to the lesser of the two p_T values, the integer n depends on the specific jet algorithm, $\Delta R_{ij} = \sqrt{(\Delta y_{ij})^2 + (\Delta\phi_{ij})^2}$ is the distance between i and j in rapidity ($y = \frac{1}{2}\ln(E+p_z)/(E-p_z)$) and azimuth ($\phi$), and R is the "size" parameter of order unity [29], with all angles expressed in radians. The particle pair (i, j) with smallest d_{ij} is combined into a single object. All distances are recalculated using the new object, and the procedure is repeated until, for a given object i, all the d_{ij} are greater than d_{iB}. Object i is then classified as a jet and not considered further in the algorithm. The process is repeated until all input particles are clustered into jets.

JHEP05(2013)090

The value for n in eqs. (2.1) and (2.2) governs the topological properties of the jets. For $n = 1$ the procedure is referred to as the k_T algorithm (KT). The KT jets tend to have irregular shapes and are especially useful for reconstructing jets of lower momentum [29]. For this reason, they are also sensitive to the presence of low-p_T pileup (PU) contributions, and are used to compute the mean p_T per unit area (in (y, ϕ)) of an event [30]. For $n = -1$, the procedure is called the anti-k_T (AK) algorithm, with features close to an idealized cone algorithm. The AK algorithm is used extensively in LHC experiments and by the theoretical community for finding well-separated jets [29]. For $n = 0$, the procedure is called the Cambridge-Aachen (CA) algorithm. This relies only on angular information, and, like the k_T algorithm, provides irregularly-shaped jets in (y, ϕ). The CA algorithm is useful in identifying jet substructure [31–33].

Jet grooming techniques [26] that reduce the impact of contributions from the underlying event (UE), PU, and low-p_T gluon radiation can be useful irrespective of the specific nature of analysis. These kinds of contributions to jets are typically soft and diffuse, and hence contribute energy to the jet proportional to the area [30]. Because grooming techniques reduce the areas of jets without affecting the core components, the resulting jets are less sensitive to contributions from UE and PU, while still reflecting the kinematics of the hard original process. We consider three forms of grooming, referred to as filtering, trimming, and pruning. Such techniques can be applied to jets clustered through different algorithms (KT, AK, or CA). For the dijet analysis, we choose to cluster jets with the anti-k_T algorithm with $R = 0.7$ (AK7), as these are used extensively at CMS. For the V+jet analysis, in addition to AK7 jets, we also study CA jets with $R = 0.8$ (CA8), considered in recent publications involving top-quark tagging [34], and with $R = 1.2$ (CA12), which was proposed for analyses involving highly-boosted objects [24]. After the initial jet clustering with AK7, CA8, or CA12, the constituents of those jets are reclustered with a (possibly different) jet algorithm (e.g., KT, CA, or AK), applying additional grooming conditions to the sequence of selection criteria used for clustering. The optimal choice of this secondary clustering algorithm depends on the grooming technique, as described below. For the techniques we have investigated, the parameters chosen for the algorithms correspond to those chosen by refs. [24–27], nevertheless specific optimization would appear to be advisable for all well-defined searches for new phenomena.

2.2 Filtering algorithm

The "mass-drop/filtering" procedure aims to identify symmetric splitting of jets of large p_T that have large m_J values. It was proposed initially for use in searches for the Higgs boson [24], but we consider just the filtering aspects of this algorithm for grooming jets.

For each jet obtained in the initial clustering procedure, the filtering algorithm defines a new, groomed jet through the following algorithm: (i) the constituents of each jet are reclustered using the CA algorithm with $R = 0.3$, thereby defining n new subjets $s_1, \ldots, s_n$, ordered in descending p_T, and (ii) the four-momentum of the new jet is defined by the four-vector sum over the three subjets of hardest p_T, or in the rare case that $n < 3$, just these remaining subjets define the new jet.

JHEP05(2013)090

The new jet has fewer particles than the initial jet, thereby reducing the contribution from effects such as underlying event and pileup, and the new m_J and p_T values are therefore smaller than those of the initial jet. As will be demonstrated in section 2.5, with this choice of parameters, filtering removes the fewest jet constituents, and is therefore the least aggressive of the investigated jet grooming techniques.

2.3 Trimming algorithm

Trimming ignores particles within a jet that fall below a dynamic threshold in p_T [25]. It reclusters the jet's constituents using the k_T algorithm with a radius R_{sub}, accepting only the subjets that have $p_{T\,sub} > f_{cut}\lambda_{hard}$, where f_{cut} is a dimensionless cutoff parameter, and λ_{hard} is some hard QCD scale chosen to equal the p_T of the original jet. The R_{sub} and f_{cut} parameters of the algorithm are taken to be 0.2 and 0.03, respectively. As will be demonstrated, with this choice of parameters, trimming removes more jet constituents than the filtering procedure, but fewer jet constituents than pruning, and corresponds therefore to a moderately aggressive jet grooming technique.

2.4 Pruning algorithm

Following the clustering of jets using the original algorithm (either AK7, CA8, or CA12), the pruning algorithm [26, 27] reclusters the constituents of the jet through the CA algorithm, using the same distance parameter, but additional conditions beyond those given in eq. (2.1). In particular, the softer of the two particles i and j to be merged is removed when the following conditions are met:

$$z_{ij} = \frac{\min(p_{Ti}, p_{Tj})}{p_{Ti} + p_{Tj}} < z_{cut} \tag{2.3}$$

$$\Delta R_{ij} > D_{cut} \equiv \alpha \cdot 2\frac{m_J}{p_T}, \tag{2.4}$$

where m_J and p_T are the mass and transverse momentum of the originally-clustered jet, and z_{cut} and α are parameters of the algorithm, chosen to be 0.1 and 0.5, respectively. In our particular choice of parameters, we have chosen to divide the jet into two "exclusive" subjets (similarly to the exclusive k_T algorithm [29], where one clusters constituents until the jets are all separated by the parameter R in eq. 2.1). As will be demonstrated, with this choice of parameters, pruning removes the largest number of jet constituents, and can therefore be regarded as the most aggressive jet grooming technique investigated. It was previously used in the CMS search for $t\bar{t}$ resonances [34].

2.5 Groomed jet mass

Figure 1 shows a comparison of distributions in the dijet sample for the ratio of groomed AK7 jet mass to the mass of the matched ungroomed AK7 jet, for our three grooming techniques, for data and for PYTHIA6 MC simulation [35], using the Z2 tune. Three distributions are shown for each grooming technique: (i) the reconstructed data ("data RECO"), (ii) the reconstructed simulated PYTHIA6 data ("PYTHIA RECO"), and (iii) the generated

JHEP05(2013)090

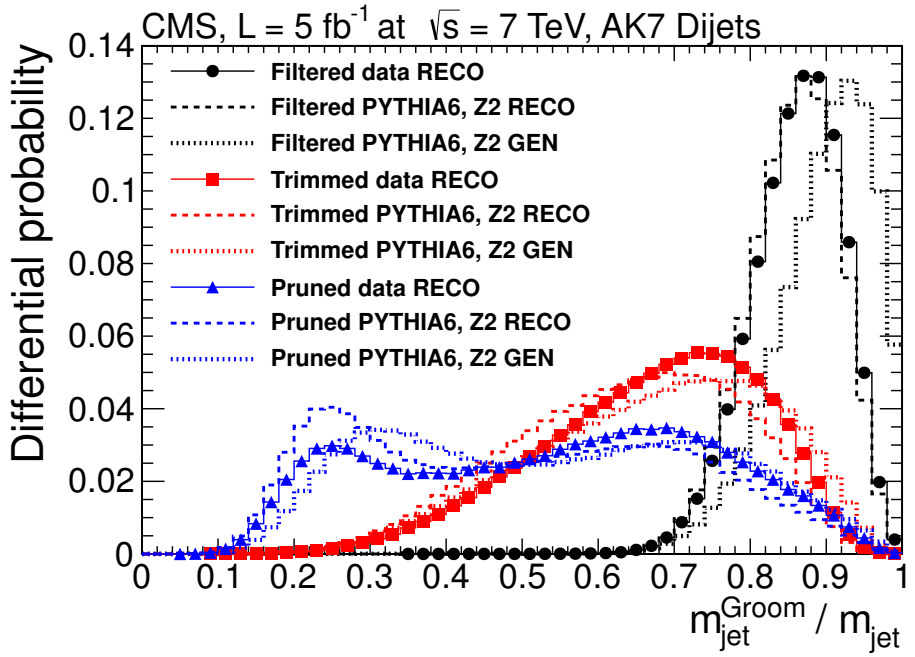

Figure 1. Distributions in differential probability for ratios of the jet mass of groomed jets to their corresponding ungroomed values, for both dijet data and PYTHIA6 (tune Z2) MC simulation, for the three grooming techniques discussed in the text: (i) filtering (circles, peaking near 0.9), (ii) trimming (squares, peaking near 0.75), and (iii) pruning (triangles, more dispersed).

particle-level jets from PYTHIA6 ("PYTHIA GEN"). These three grooming techniques involve different jet algorithms for grooming (CA for filtering and pruning, k_T for trimming) once the jets are found with AK7. The data and the simulation exhibit similar behavior. In general, the filtering algorithm is the least aggressive grooming technique, with groomed jet masses close to the ungroomed values. The trimming algorithm is moderately aggressive, and the pruning algorithm is the most aggressive of the three. With pruning, a bimodal distribution begins to appear, which is typical of our implementation of this algorithm as we require clustering into two exclusive subjets. In cases where the pruned jet mass is small, jets usually have most of their energy configured in "core" components, with little gluon radiation, which leads to narrow jets. When the pruned jet mass is large, the jets are split more symmetrically, which can be realized in events with gluons splitting into two nodes that fall within $\Delta R = 0.7$ of the original parton.

3 The CMS detector and simulation

The CMS detector [36] is a general-purpose device with many features suited for reconstruction of energetic jets, specifically, the finely segmented electromagnetic and hadronic calorimeters and charged-particle tracking detectors.

CMS uses a right-handed coordinate system, with origin defined by the center of the CMS detector, the x axis pointing to the center of the LHC ring, the y axis pointing up, perpendicular to the plane of the LHC ring, and the z axis along the direction of the

JHEP05(2013)090

counterclockwise beam. The polar angle θ is measured relative to the positive z axis and the azimuthal angle ϕ relative to the x axis in the x-y plane.

Charged particles are reconstructed in the inner silicon tracker, which is immersed in a 3.8 T axial magnetic field. The CMS tracking detector consists of an inner silicon pixel detector composed of three concentric central layers and two sets of disks arranged forward and backward of the center, and up to ten silicon strip central layers and three inner and nine outer strip disks forward and backward of the center. This arrangement provides full azimuthal coverage for $|\eta| < 2.5$, where $\eta = -\ln[\tan(\theta/2)]$ is the pseudorapidity. The pseudorapidity approximates the rapidity y and equals y for massless particles. Since many of the reconstructed jets are not massless, we use the rapidity y for characterizing jets in this analysis.

A lead tungstate crystal electromagnetic calorimeter (ECAL) and a brass/scintillator hadronic calorimeter (HCAL) surround the tracking volume and provide photon, electron, and jet reconstruction up to $|\eta| = 3$. The ECAL and HCAL cells are grouped into towers projecting radially outward from the center of the detector. In the central region ($|\eta| < 1.74$), the towers have dimensions of $\Delta\eta = \Delta\phi = 0.087$ that increase at larger $|\eta|$. ECAL and HCAL cell energies above some chosen noise-suppression thresholds are combined within each tower to define the tower energy. Muons are measured in gas-ionization detectors embedded in the steel return yoke outside the solenoid. To improve reconstruction of jets, the tracking and calorimeter information is combined in a "particle-flow" (PF) algorithm [37], which is described in section 4.4.

For the analysis of dijet events, samples are simulated with PYTHIA6.4 (Tune Z2) [35, 38], PYTHIA8 (Tune 4c) [39], and HERWIG++ (Tune 23) [40], and propagated through the simulation of the CMS detector based on GEANT4 [41]. Underlying event (UE) and pileup (PU) are included in the simulations, which are also reweighted to have the simulated PU distribution match the observed PU distribution in the data.

For the V+jet analysis, events with a vector boson produced in association with jets are simulated using MADGRAPH 5.1 [42]. This matrix element generator is also used to simulate $t\bar{t}$ events. The MADGRAPH events are subsequently subjected to parton showering, simulated with PYTHIA6 using the Z2 Tune [38]. To compare hadronization in different generators, we generate V+jet samples in which parton showering and hadronization are simulated with HERWIG++. Diboson (WW, WZ, and ZZ) events are also generated with PYTHIA6. Single-top-quark samples are produced with POWHEG [43], and the lepton enriched dijet samples are produced with PYTHIA6 using the Z2 Tune. CTEQ6L1 [44] is the default set of parton distribution functions used in all these samples, except for the single-top-quark MC, which uses CTEQ6M.

4 Triggers and event reconstruction

4.1 Dijet trigger selection

Events are collected using single-jet triggers, which are based on jets reconstructed only from calorimetric information. This procedure yields inferior resolution to jets reconstructed offline with PF constituents, but provides faster reconstruction that meets trig-

JHEP05(2013)090

Trigger p_{T} threshold (GeV)	$p_{\mathrm{T}}^{\mathrm{AVG}}$ range (GeV)
190	220–300
240	300–450
370	>450

Table 1. Trigger p_{T} thresholds for individual jets, and corresponding $p_{\mathrm{T}}^{\mathrm{AVG}}$ intervals used to assign the triggered events in the dijet analysis.

ger requirements. As the instantaneous luminosity is time-dependent, the specific jet-p_{T} thresholds change with time. The triggers used to select dijet events have partial overlap. Those with lower-p_{T} thresholds have high prescale settings to accommodate the higher data-acquisition rates, and some events selected with these lower-p_{T} triggers are also collected at higher thresholds.

To avoid double counting of phase space, each event is assigned to a specific trigger. To do this, we compute the trigger efficiency as a function of reconstructed $p_{\mathrm{T}}^{\mathrm{AVG}}$, select an interval in trigger efficiency where the efficiency is maximum (>95%) for that range of $p_{\mathrm{T}}^{\mathrm{AVG}}$, and assign that trigger to the appropriate $p_{\mathrm{T}}^{\mathrm{AVG}}$ interval. The assignment is based on the jet p_{T} values reconstructed offline (but not groomed). Table 1 shows the p_{T} thresholds for each of the jet triggers used in the analysis, and the corresponding intervals of p_{T} to which the triggered events are assigned.

4.2 V+jet trigger selection

Several triggers are also used to collect events corresponding to the topology of V+jet events, where the V decays via electrons or muons in the final state. For the W+jet channels, the triggers consist of several single-lepton triggers, with lepton identification criteria applied online. To assure an acceptable event rate, leptons are required to be isolated from other tracks and energy depositions in the calorimeters. For the W($\mu\nu_{\mu}$) channel, the trigger thresholds for the muon p_{T} are in the range of 17 to 40 GeV. The higher thresholds are used at higher instantaneous luminosity. The combined trigger efficiency for signal events that pass offline requirements (described in section 5) is ≈92%.

For the W($\mathrm{e}\nu_{\mathrm{e}}$) events, the electron p_{T} threshold ranges from 25 to 65 GeV. To enhance the fraction of W+jet events in the data, the single-electron triggers are also required to have minimum thresholds on the magnitude of the imbalance in transverse energy ($E_{\mathrm{T}}^{\mathrm{miss}}$) and on the transverse mass (m_{T}) of the (electron + $E_{\mathrm{T}}^{\mathrm{miss}}$) system, where $m_{\mathrm{T}}^2 = 2E_{\mathrm{T}}^{\mathrm{e}}E_{\mathrm{T}}^{\mathrm{miss}}(1-\cos\phi)$, and ϕ is the angle between the directions of $p_{\mathrm{T}}^{\mathrm{e}}$ and $E_{\mathrm{T}}^{\mathrm{miss}}$. The combined efficiency for electron W+jet events that pass the offline criteria is ≈99%.

The Z($\mu\mu$) channel uses the same single-muon triggers as the W($\mu\nu_{\mu}$) channel. The Z(ee) channel uses dielectron triggers with lower thresholds for p_{T} (17 and 8 GeV), and additional isolation requirements. These triggers are 99% efficient for all Z+jet events that pass the final offline selection criteria.

JHEP05(2013)090

Bin	p_T interval (GeV)	Analysis
1	125–150	V + jet
2	150–220	V + jet
3	220–300	V + jet,dijet
4	300–450	V + jet,dijet
5	450–500	dijet
6	500–600	dijet
7	600–800	dijet
8	800–1000	dijet
9	1000–1500	dijet

Table 2. Intervals in ungroomed jet p_T for the V+jet and dijet analyses.

4.3 Binning jets as a function of p_T

The jet p_T bins introduced in eq. (1.1) are given in table 2 for V+jet and dijet events. The jet p_T is re-evaluated for each grooming algorithm. Because there are large biases due to jet misassignment in the dijet events, especially at small p_T (when three particle-level jets are often reconstructed as two jets in the detector, or vice versa), the p_T intervals for these events begin at 220 GeV. Furthermore, the smaller number of events in the V+jet samples precludes the study of these events beyond $p_T = 450$ GeV.

4.4 Event reconstruction

As indicated above, events are reconstructed using the particle-flow algorithm, which combines the information from all subdetectors to reconstruct the particle candidates in an event. The algorithm categorizes particles into muons, electrons, photons, charged hadrons, and neutral hadrons. The resulting PF candidates are passed through each jet clustering algorithm of section 2, as implemented in FastJet (Version 3.0.1) [45, 46].

The reconstructed interaction vertex characterized by the largest value of $\sum_i (p_{T_i}^{trk})^2$, where $p_{T_i}^{trk}$ is the transverse momentum of the i^{th} charged track associated with the vertex, is defined as the leading primary vertex (PV) of the event. This vertex is used as the reference vertex for all PF objects in the event. A pileup interaction can affect the reconstruction of jet momenta and E_T^{miss}, as well as lepton isolation and b-tagging efficiency. To mitigate these effects, a track-based algorithm is used to remove all charged hadrons that are not consistent with originating from the leading PV.

Electron reconstruction requires the matching of an energy cluster in the ECAL with a track extrapolated from the silicon tracker [47]. Identification criteria based on the energy distribution of showers in the ECAL and consistency of tracks with the primary vertex are imposed on electron candidates. Additional requirements remove any electrons produced through conversions of photons in detector material. The analysis considers electrons only in the range of $|\eta| < 2.5$, excluding the transition region $1.44 < |\eta| < 1.57$ between the central and endcap ECAL detectors because of poorer resolution for electrons in this region. Muons are reconstructed using two algorithms [48]: (i) in which tracks in the silicon tracker

JHEP05(2013)090

are matched to signals in the muon chambers, and (ii) in which a global fit is performed to a track seeded by signals in the external muon system. The muon candidates are required to be reconstructed through both algorithms. Additional identification criteria are imposed on muon candidates to reduce the fraction of tracks misidentified as muons, and to reduce contamination from muon decays in flight. These criteria include the number of hits detected in the tracker and in the outer muon system, the quality of the fit to a muon track, and its consistency of originating from the leading PV.

Charged leptons from V-boson decays are expected to be isolated from other energy depositions in the event. For each lepton candidate, a cone with radius 0.3 for muons and 0.4 for electrons is chosen around the direction of the track at the event vertex. When the scalar sum of the transverse momenta of reconstructed particles within that cone, excluding the contribution from the lepton candidate, exceeds ≈10% of the p_T of the lepton candidate, that lepton is ignored. The exact isolation requirement depends on the η, p_T, and flavor of the lepton. Muons and electrons are required to have $p_T > 30\,\text{GeV}$ and $> 80\,\text{GeV}$, respectively. The large threshold for electrons ensures good trigger efficiency. To avoid double counting, isolated charged leptons are removed from the list of PF objects that are clustered into jets.

After removal of isolated leptons and charged hadrons from pileup vertices, only the neutral hadron component from pileup remains and is included in the jet clustering. This remaining component of pileup to the jet energy is removed by applying a correction based on a mean p_T per unit area of $(\Delta y \times \Delta\phi)$ originating from neutral particles [30, 49]. This quantity is computed using the k_T algorithm, and corrects the jet energy by the amount of energy expected from pileup in the jet cone. This "active area" method adds a large number of soft "ghost" particles to the clustering sequence to determine the effective area subtended by each jet. This procedure is done for all grooming algorithms just as for the ungroomed jets. The active area of a groomed jet is smaller than that of an ungroomed jet, and the pileup correction is therefore also smaller. Different responses in the endcap and central barrel calorimeters necessitate using η-dependent jet corrections. The amount of energy expected from the remnants of the hard collision (the underlying event) is estimated from minimum-bias data and MC events, and is added back into the jet.

In addition, the pileup-subtracted jet four-momenta in data are corrected for nonlinearities in η and p_T by using a p_T- and η-dependent correction to account for the difference between the response in MC-simulated events and data [50]. The jet corrections are derived for the ungroomed jet algorithms but are also applied to the groomed algorithms, thereby adding additional systematic uncertainty in the energy of groomed jets.

5 Event selection

We apply several other selection criteria to minimize instrumental background and electronic noise. In particular, accepted events must have at least one good primary vertex (section 4.4). Backgrounds from additional beam interactions are reduced by applying a variety of requirements on charged tracks. Finally, calorimeter noise is minimized through restrictions on timing and electronic pulse shapes expected for signals.

JHEP05(2013)090

Dijet events are required to have at least two AK7 jets, each with $p_{\mathrm{T}} > 50\,\mathrm{GeV}$ and $|y| < 2.5$, and each jet must satisfy the jet quality criteria discussed in ref. [37]. No third-jet veto is applied.

Reconstruction of W and Z bosons in V+jet events begins with identification of charged leptons and a calculation of $E_{\mathrm{T}}^{\mathrm{miss}}$, described in the previous section. Candidates for $\mathrm{Z} \to \ell^+\ell^-$ ($\ell = \mathrm{e}$ or μ) decays are reconstructed by combining two isolated electrons or muons and requiring the dilepton invariant mass to be in the $80 < M_{\ell\ell} < 100\,\mathrm{GeV}$ range. An accurate measurement of $E_{\mathrm{T}}^{\mathrm{miss}}$ is essential for distinguishing the W signal from background processes. The $E_{\mathrm{T}}^{\mathrm{miss}}$ in the event is defined using the PF objects, and this analysis requires $E_{\mathrm{T}}^{\mathrm{miss}} > 50\,\mathrm{GeV}$. Candidate $\mathrm{W} \to \ell\nu_\ell$ decays are identified primarily through the presence of a significant $E_{\mathrm{T}}^{\mathrm{miss}}$ and a single isolated lepton of large p_{T}, with p_{T} and m_{T} of the W candidate obtained by combining the lepton and the $E_{\mathrm{T}}^{\mathrm{miss}}$ vectors.

The analysis of V+jet events is mainly of interest for the regime of $p_{\mathrm{T}}^{\mathrm{V}} > 120\,\mathrm{GeV}$, in which the opposing jet tends to have large p_{T} as well, because of momentum conservation. In fact, the leading jet in each event (independent of clustering algorithm and jet radius) is required to have $p_{\mathrm{T}} > 125\,\mathrm{GeV}$ and $|y| < 2.5$. A back-to-back topology between the vector boson and the leading jet is ensured by the additional selection of $\Delta\phi(\mathrm{V}, \mathrm{jet}) > 2$ and $\Delta R(\ell, \mathrm{jet}) > 1$. Requiring such highly boosted jets, in addition to the tight isolation criteria for the leptons, greatly suppresses the background from multijet production. In the $\mathrm{W} \to \ell\nu_\ell$+jet analysis, additional rejection of multijet background is achieved by requiring $m_{\mathrm{T}}(\mathrm{W}) > 50\,\mathrm{GeV}$. No subleading-jet veto is applied.

Figures 2(a) and (b) show the p_{T} distributions for the leading AK7 jet selected in Z+jet and W+jet candidate events, respectively. Given the unique signature for highly-boosted vector bosons recoiling from jets, the selections suffice to define very pure samples of V+jet events. In the $\mathrm{Z}(\ell\ell)$+jet analysis, the additional constraint on dilepton mass removes almost all background contributions, yielding a purity of ≈99% for Z+jet events, with ≈1% contamination from diboson production. The W+jet candidate sample contains ≈82% W+jet events, with small background contributions from $\mathrm{t\bar{t}}$ (13%), single top-quark (3%), and diboson and Z+jet (1% each) events based on MC simulation. The small number of events expected from these processes are subtracted using MC predictions for the jet mass from the W+jet candidate events, before correcting the data for detector effects. Similarly, the small number of events expected from diboson production are subtracted from the Z +jet candidates.

6 Influence of pileup on jet grooming algorithms

During the data taking the instantaneous LHC luminosity exceeded $\approx 3.0 \times 10^{33}\,\mathrm{cm^{-2}\,s^{-1}}$, or an average of ten interactions per bunch crossing. Such pileup collisions are not correlated with the hard-scattering process that triggers an interesting event, but present a background from low-p_{T} interactions that can affect the measured energies of jets and their observed masses. Methods to mitigate these effects are part of standard event reconstruction, as discussed in section 4.4, and are essential for extracting correct jet multiplicities and energies. The jet mass is expected to be particularly sensitive to pileup [1] for jets

JHEP05(2013)090

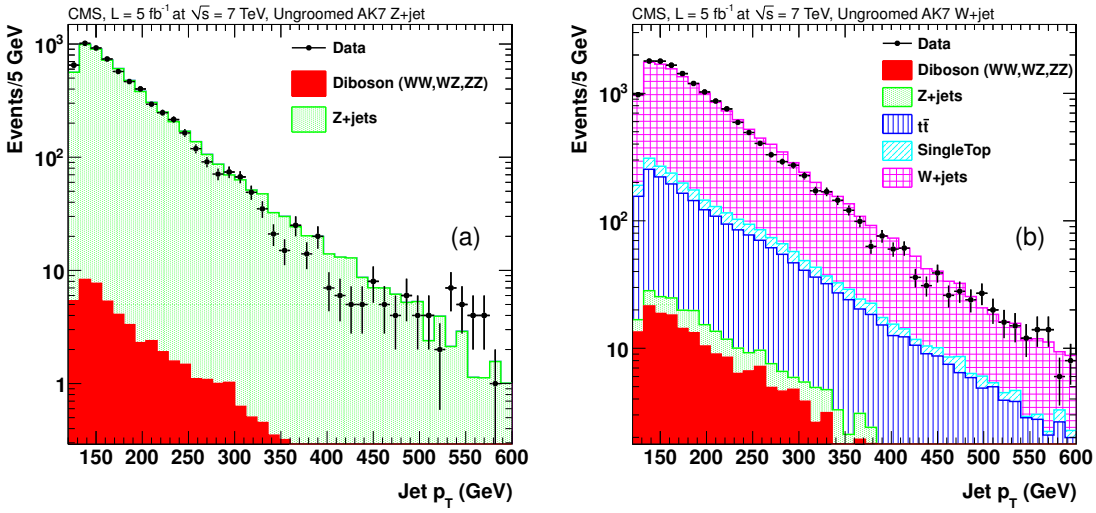

Figure 2. The p_{T} distribution for the leading AK7 jet in accepted (a) Z+jet and (b) W+jet events.

Ratio of slopes	Measured	Expected
$s_{0.7}/s_{0.5}$	$2.7 \pm 0.9\,(\mathrm{stat.})$	$(0.7/0.5)^3 = 2.74$
$s_{0.8}/s_{0.5}$	$3.3 \pm 1.0\,(\mathrm{stat.})$	$(0.8/0.5)^3 = 4.10$
$s_{0.8}/s_{0.7}$	$1.2 \pm 0.2\,(\mathrm{stat.})$	$(0.8/0.7)^3 = 1.49$

Table 3. Slopes of linear fits of $\langle m_J \rangle$ as a function of N_{PV} for AK jets of different R values.

of large angular extent that contain many particles. Grooming techniques are designed to reduce the effective area of such jets and thereby minimize sensitivity to pileup. We examine this issue through studies of jet mass in the presence of pileup.

The mean jet mass $\langle m_J \rangle$ for AK jets is presented for size parameters $R = 0.5$, 0.7, and 0.8, as a function of the total number of reconstructed primary vertices (N_{PV}) in figure 3(a), for data and MC simulation. The mean mass for $N_{\mathrm{PV}} = 1$ increases linearly with the jet radius from 0.5 to 0.8. A measure of the dependence of $\langle m_J \rangle$ on pileup is given by the slope of a linear fit to the jet mass versus N_{PV}. The ratios of these slopes (s_R) are found to be roughly consistent with the ratio of the third power of the jet radius, as summarized in table 3.

This is in agreement with predictions for scaling of the mean mass [51]. The R^3 dependence can be understood in terms of the increase of the jet area as R^2. Simultaneously, the contribution of these particles to the jet mass scales with the distance between them, or $\approx R/2$, yielding another power of R.

In figure 3(b) we show the dependence of $\langle m_J \rangle$ on N_{PV}, for AK7 jets, for different grooming algorithms. The grooming significantly reduces the impact of pileup on $\langle m_J \rangle$, as reflected by the decrease of the slope of the linear fit to the groomed-jet data points, as summarized in table 4.

The observed agreement between data and simulation in figure 3 provides support for our characterization of jet grooming and pileup, and the decrease in slopes suggests that grooming is indeed an effective tool for suppressing the impact of pileup on jets with large R parameters.

JHEP05(2013)090

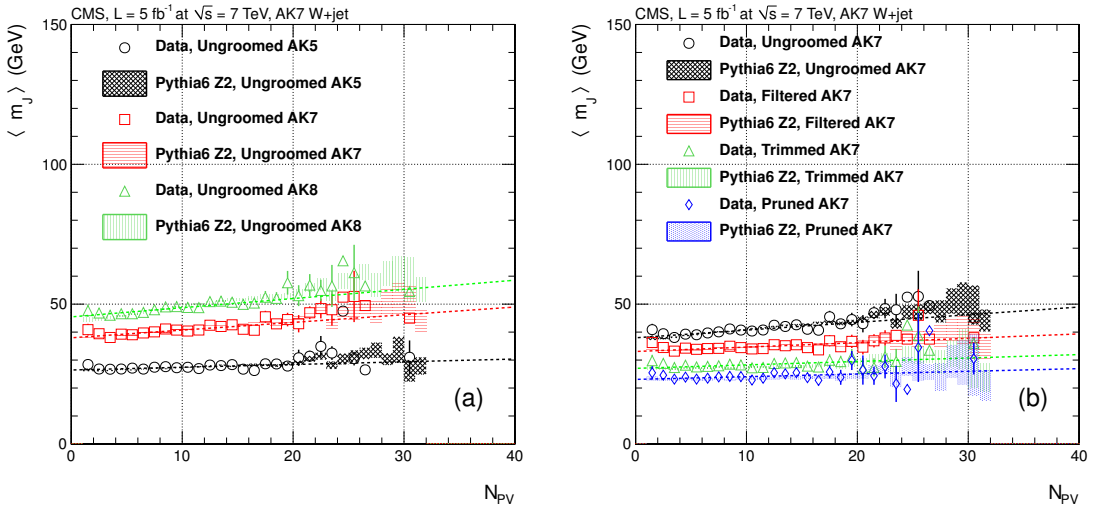

Figure 3. Distributions of the average jet mass for AK jets as a function of the number of reconstructed primary vertices: (a) for different jet radii, and (b) for AK7 jets, comparing the impact of grooming algorithms to results without grooming.

Jet R	Clustering algorithm	s_R (GeV/PV)
AK5	ungroomed	0.10 ± 0.03 (stat.)
AK7	ungroomed	0.28 ± 0.03 (stat.)
AK7	filtered	0.16 ± 0.02 (stat.)
AK7	trimmed	0.12 ± 0.04 (stat.)
AK7	pruned	0.10 ± 0.05 (stat.)
AK8	ungroomed	0.33 ± 0.03 (stat.)

Table 4. Values of slopes for the dependence of $\langle m_J \rangle$ on N_{PV} for AK jets with different radii and clustering algorithms.

7 Corrections and systematic uncertainties

Before comparison of the jet mass distributions with QCD predictions, the data are corrected to the particle level for detector effects, such as resolution and acceptance. The simulated particle-level jets are reconstructed with the same algorithm and with the same parameters as the PF jets. We use the unfolding procedure described in refs. [52–56] to correct the jet mass, through an iterative technique for finding the maximum-likelihood solution of the unfolding problem. The detector response matrix is obtained in MC studies of jets. In general, the number of iterations must be tuned to minimize the impact of statistical fluctuations on the result. In practice, however, the procedure is largely insensitive to the precise settings and binning of events and four iterations usually suffice. A larger number of iterations were found to provide the same results except for small fluctuations in the tails of distributions. A simpler bin-by-bin unfolding is used as a cross-check, and is found to provide similar results, with fluctuations in the tails of the distributions. The jet transverse momenta are not unfolded.

JHEP05(2013)090

Systematic uncertainties are estimated by modifying the response matrix for each source of uncertainty by ±1 standard deviation, and comparing the mass distribution to the nominal results, based on simulated PYTHIA6 events. The difference in the unfolded mass spectrum from such a change is taken as the uncertainty arising from that source.

The experimental uncertainties that can affect the unfolding of the jet mass include the jet energy scale (JES), jet energy resolution (JER), and jet angular resolution (JAR). The uncertainty from JES is estimated by raising and lowering the jet four-momenta by the measured uncertainty as a function of jet p_{T} and η [50], which typically corresponds to 1–2% for the jets in this analysis. Two additional p_{T}- and η-independent uncertainties are included: a 1% uncertainty to account for differences observed between the measured and predicted W mass for high-p_{T} jets in a $\mathrm{t\bar{t}}$-enriched sample, and a 3% uncertainty to account for differences in the groomed and ungroomed energy responses found in MC simulation [34].

The impact of uncertainties in JER and JAR on m_J are evaluated by smearing the jet energies, as well as the resolutions in η and ϕ, each by 10% in the MC simulation relative to the particle-level generated jets [50]. These estimated uncertainties on JER and JAR are found to be essentially the same for all jet grooming techniques in MC studies. Since this analysis uses jets constructed from PF constituents, the charged particles have excellent energy and angular resolutions, but their use induces a dependence on tracking uncertainties, e.g., tracking efficiency. This dependence is accounted for implicitly in the ±10% changes in jet energy and angular resolutions, since such changes would lead to a difference between expected and observed values of these quantities. The same is true for the neutral electromagnetic component of the jet (primarily from $\pi^0 \to \gamma\gamma$ decays).

The remaining sources of uncertainty are estimated from MC simulation. The tracking information is not sensitive to the neutral hadronic component of jets, and this small contribution is taken directly from simulation. We estimate this remaining uncertainty by comparing the unfolded data using PYTHIA6 and using HERWIG++, and assign the difference as a systematic uncertainty. This also accounts for the uncertainty from modeling parton showers. The latter effect often comprises the largest uncertainty in the unfolded jet mass distributions as described below. Other theoretical ambiguities that can affect the unfolding of the jet mass include the variation of the parton distribution functions and the modeling of initial and final-state radiation (ISR/FSR). The former was investigated and found to be much smaller than the difference between the unfolding with PYTHIA6 and the unfolding with HERWIG++, and hence is neglected. The latter is included implicitly in the uncertainty between PYTHIA6 and HERWIG++.

As described in section 4.4, the jets used in this analysis are reconstructed after removing the charged hadrons that appear to emanate from subleading primary vertices. This procedure produces a dramatic (≈60%) reduction in the pileup contribution to jets. The residual uncertainty from pileup is obtained through MC simulation, estimated by increasing and decreasing the cross section for minimum-bias events by 8%.

In the dijet analysis, there can be incorrect assignments of leading reconstructed jets relative to the generator level, e.g., two generator-level jets can be matched to three reconstructed jets, or vice versa. This effect causes a bias in the unfolding procedure, which becomes greater at small p_{T}. This bias is corrected through MC studies of matching of

JHEP05(2013)090

particle-level jets to reconstructed jets, and the magnitude of the bias correction is also added to the overall systematic uncertainty. Such misassignments are negligible in the V+jet analysis.

8 Results from dijet final states

The differential probability distributions of eq. (1.2) for m_J^{AVG} of the two leading jets in dijet events, corrected for detector effects in the jet mass, are displayed in figures 4–7 for seven bins in $p_{\mathrm{T}}^{\mathrm{AVG}}$ along with the HERWIG++ predictions. The $p_{\mathrm{T}}^{\mathrm{AVG}}$ is not corrected to the particle level, because the correction is expected to be negligible for the momenta considered. Results are shown for ungroomed jets and for the three categories of grooming. Each distribution is normalized to unity. The ratios of the MC simulations used in figures 4–7 to the results for data, for PYTHIA6, PYTHIA8, and for HERWIG++ are given in figures 8–11, respectively.

The largest systematic uncertainty is from the choice of parton-shower modeling used to calculate detector corrections, with small, but still significant uncertainties arising from jet energy scale and resolution, and small contributions from jet angular resolution and pileup. In the 220–300 GeV and 300–450 GeV jet-p_{T} bins, the $m_J < 50$ GeV region is dominated by uncertainties from unfolding (50–100%), which are negligible for $p_{\mathrm{T}}^{\mathrm{AVG}} > 450$ GeV. For $m_J > 50$ GeV, the JES, JER, JAR, and pileup uncertainties each contribute ≈10%. For the 450–1000 GeV p_{T} bins, parton showering dominates the uncertainties, which is around 50–100% below the peak of the m_J distribution and 5–10% for the rest of the distribution. For $p_{\mathrm{T}} > 1000$ GeV, statistical uncertainty dominates the entire mass range.

For clarity, the distributions in figures 8–11 are truncated where few events are recorded. Bins in m_J^{AVG} with uncertainties of $> 100\%$ are ignored to avoid overlap with more precise measurements in other $p_{\mathrm{T}}^{\mathrm{AVG}}$ bins. The agreement with HERWIG++ modeling of parton showers appears to be best for $p_{\mathrm{T}}^{\mathrm{AVG}} > 300$ GeV and $m_J^{\mathrm{AVG}} > 20$ GeV. However, the ungroomed and filtered jets show worse agreement for $20 < m_J^{\mathrm{AVG}} < 50$ GeV when $p_{\mathrm{T}}^{\mathrm{AVG}} > 450$ GeV. For all generators and all $p_{\mathrm{T}}^{\mathrm{AVG}}$ bins, the agreement is better at larger jet masses. The disagreement is largest at the very lowest mass values, which correspond to the region most sensitive to the underlying event description and pileup, and where the amount of showering is apparently underestimated in the simulation.

9 Results from V+jet final states

This section provides the probability density distributions as functions of the mass of the leading jet in V+jet events. These distributions are corrected for detector effects in the jet mass, and are compared to MC expectations from MadGraph (interfaced to PYTHIA6) and HERWIG++. The jet mass distributions are studied in different ranges of p_{T} between 125 and 450 GeV, as given in table 2. (Just as in the dijet results, p_{T} is not corrected to the particle level.) For jets reconstructed with the CA algorithm ($R = 1.2$), we study only the events with $p_{\mathrm{T}} > 150$ GeV, which is most interesting for heavy particle searches in the highly-boosted regime, where all decay products are contained within $R = 1.2$ jets [24].

JHEP05(2013)090

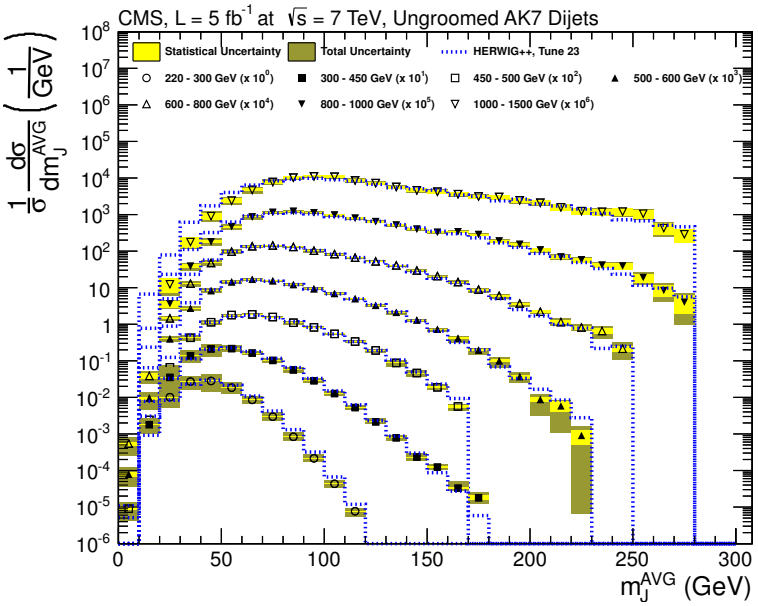

Figure 4. Unfolded distributions for the mean mass of the two leading jets in dijet events for reconstructed AK7 jets, separated according to intervals in $p_{\mathrm{T}}^{\mathrm{AVG}}$ (the mean p_{T} of the two jets). The data are shown by the symbols indicating different bins in the mean p_{T} of the two jets. The statistical uncertainty is shown in light shading, and the total uncertainty in dark shading. Predictions from HERWIG++ are given by the dotted lines. To enhance visibility, the distributions for larger values of $p_{\mathrm{T}}^{\mathrm{AVG}}$ are scaled up by the factors given in the legend.

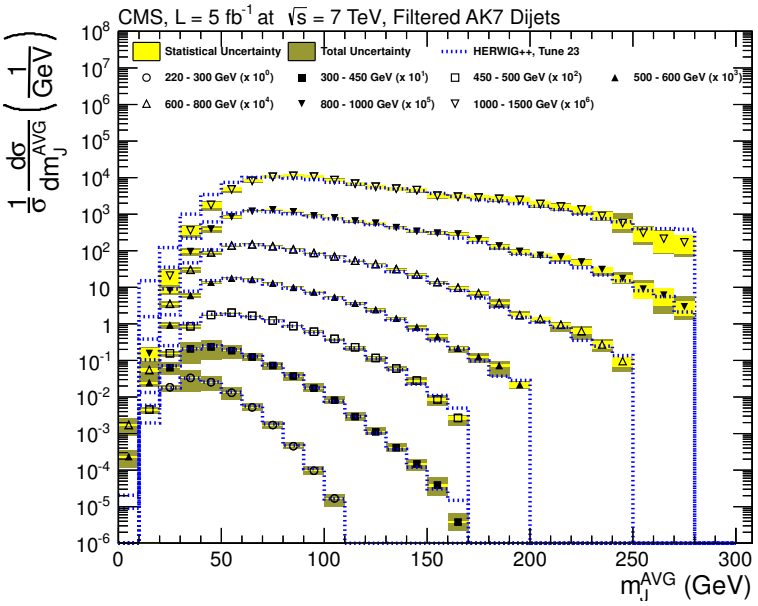

Figure 5. Unfolded distributions for the mean mass of the two leading jets in dijet events for reconstructed filtered AK7 jets, separated according to intervals in $p_{\mathrm{T}}^{\mathrm{AVG}}$ (the mean p_{T} of the two jets). The data are shown by the symbols indicating different bins in the mean p_{T} of the two jets. The statistical uncertainty is shown in light shading, and the total uncertainty in dark shading. Predictions from HERWIG++ are given by the dotted lines. To enhance visibility, the distributions for larger values of $p_{\mathrm{T}}^{\mathrm{AVG}}$ are scaled up by the factors given in the legend.

JHEP05(2013)090

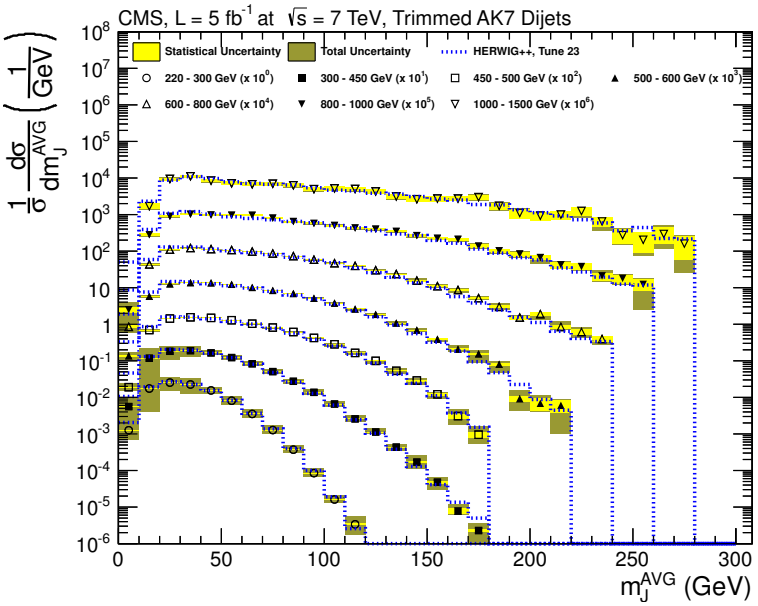

Figure 6. Unfolded distributions for the mean mass of the two leading jets in dijet events for reconstructed trimmed AK7 jets, separated according to intervals in $p_{\mathrm{T}}^{\mathrm{AVG}}$ (the mean p_{T} of the two jets). The data are shown by the symbols indicating different bins in the mean p_{T} of the two jets. The statistical uncertainty is shown in light shading, and the total uncertainty in dark shading. Predictions from HERWIG++ are given by the dotted lines. To enhance visibility, the distributions for larger values of $p_{\mathrm{T}}^{\mathrm{AVG}}$ are scaled up by the factors given in the legend.

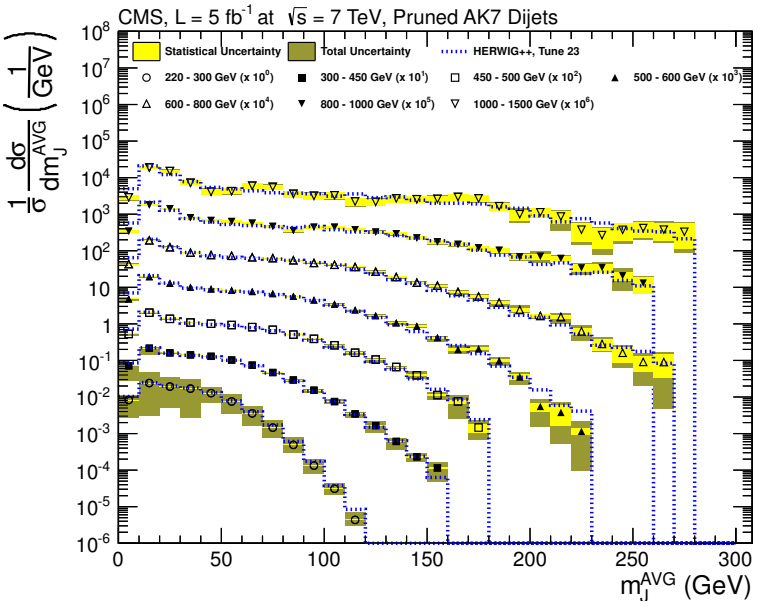

Figure 7. Unfolded distributions for the mean mass of the two leading jets in dijet events for reconstructed pruned AK7 jets, separated according to intervals in $p_{\mathrm{T}}^{\mathrm{AVG}}$ (the mean p_{T} of the two jets). The data are shown by the symbols indicating different bins in the mean p_{T} of the two jets. The statistical uncertainty is shown in light shading, and the total uncertainty in dark shading. Predictions from HERWIG++ are given by the dotted lines. To enhance visibility, the distributions for larger values of $p_{\mathrm{T}}^{\mathrm{AVG}}$ are scaled up by the factors given in the legend.

JHEP05(2013)090

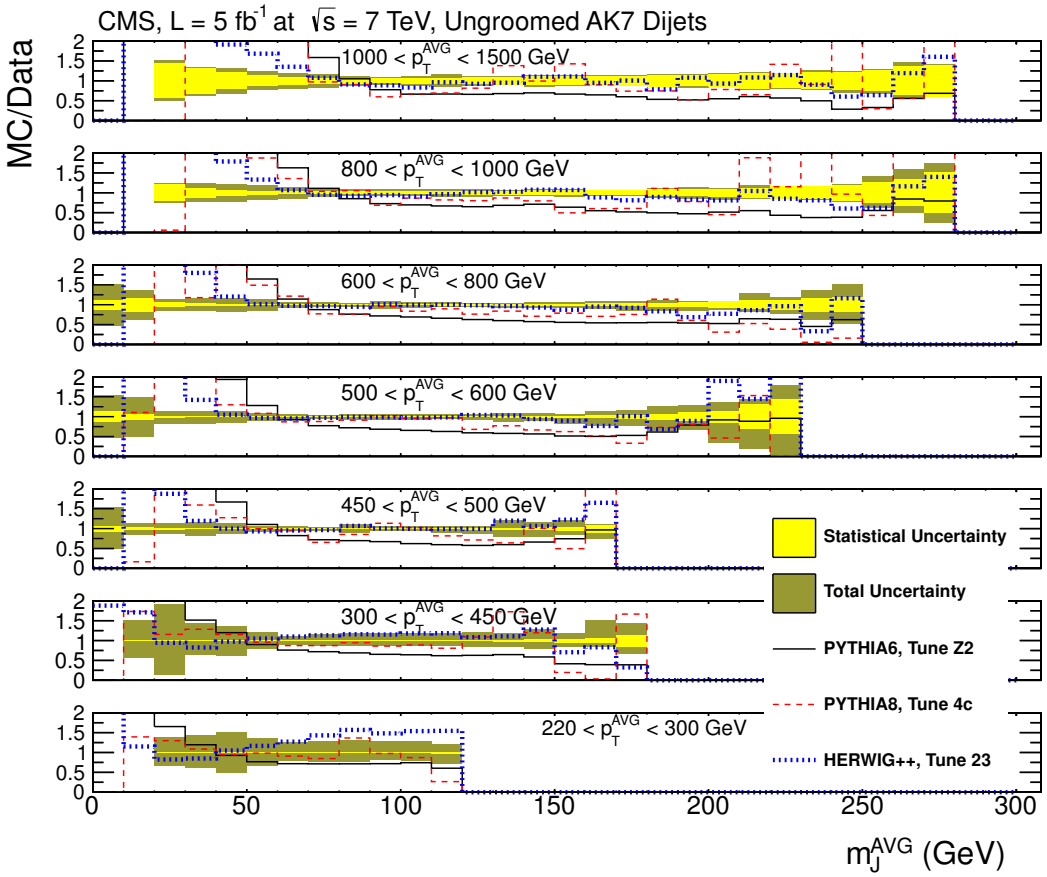

Figure 8. Ratio of MC simulation to unfolded distributions of the jet mass for AK7 jets for the seven bins in $p_{\mathrm{T}}^{\mathrm{AVG}}$. The statistical uncertainty is shown in light shading, and the total uncertainty is shown in dark shading. The comparison for PYTHIA6 is shown in solid lines, for PYTHIA8 in dashed lines, and for HERWIG++ in dotted lines.

JHEP05(2013)090

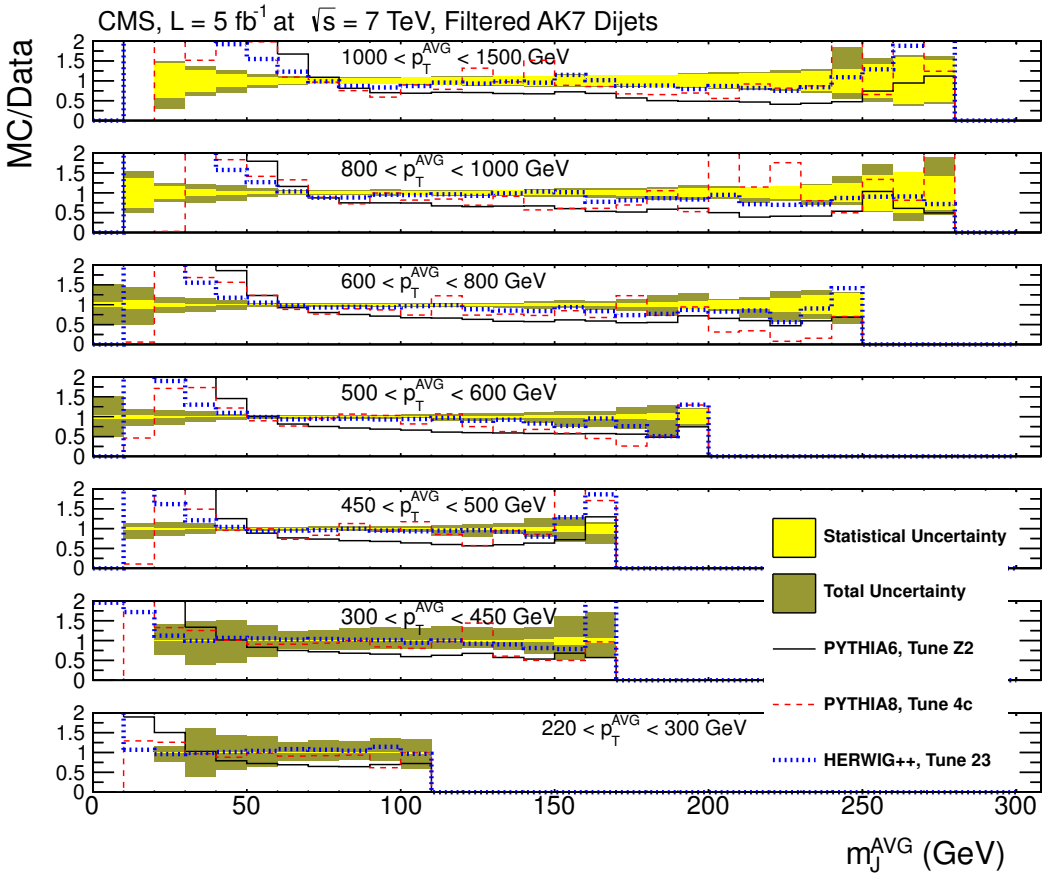

Figure 9. Ratio of MC simulation to unfolded distributions of the jet mass for filtered AK7 jets for the seven bins in $p_{\mathrm{T}}^{\mathrm{AVG}}$. The statistical uncertainty is shown in light shading, and the total uncertainty is shown in dark shading. The comparison for PYTHIA6 is shown in solid lines, for PYTHIA8 in dashed lines, and for HERWIG++ in dotted lines.

JHEP05(2013)090

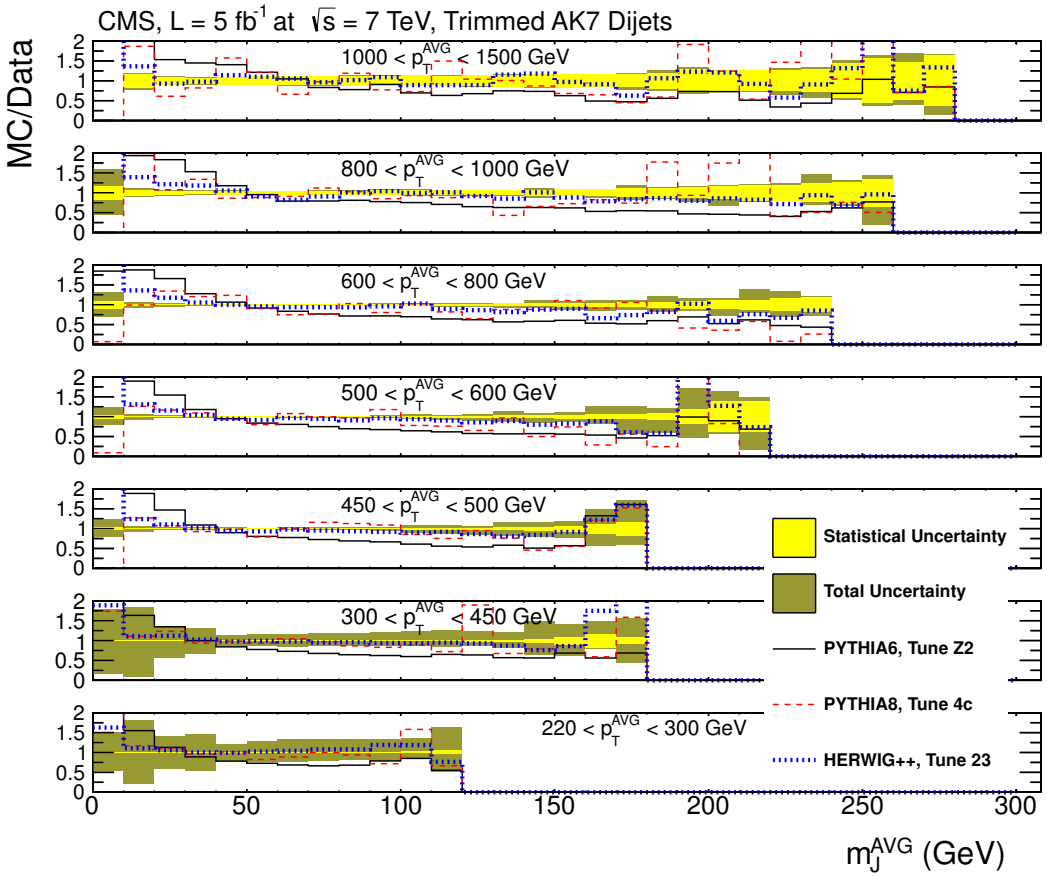

Figure 10. Ratio of MC simulation to unfolded distributions of the jet mass for trimmed AK7 jets for the seven bins in $p_{\mathrm{T}}^{\mathrm{AVG}}$. The statistical uncertainty is shown in light shading, and the total uncertainty is shown in dark shading. The comparison for PYTHIA6 is shown in solid lines, for PYTHIA8 in dashed lines, and for HERWIG++ in dotted lines.

JHEP05(2013)090

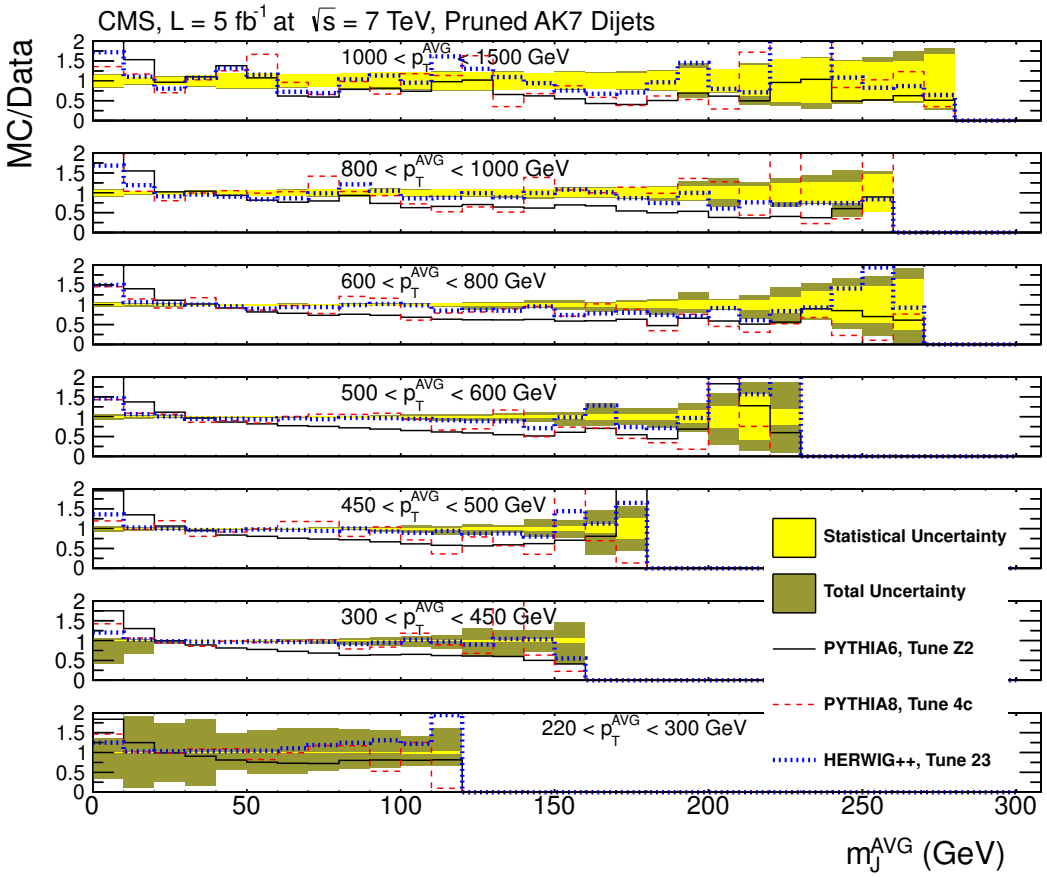

Figure 11. Ratio of MC simulation to unfolded distributions of the jet mass for pruned AK7 jets for the seven bins in $p_{\mathrm{T}}^{\mathrm{AVG}}$. The statistical uncertainty is shown in light shading, and the total uncertainty is shown in dark shading. The comparison for PYTHIA6 is shown in solid lines, for PYTHIA8 in dashed lines, and for HERWIG++ in dotted lines.

JHEP05(2013)090

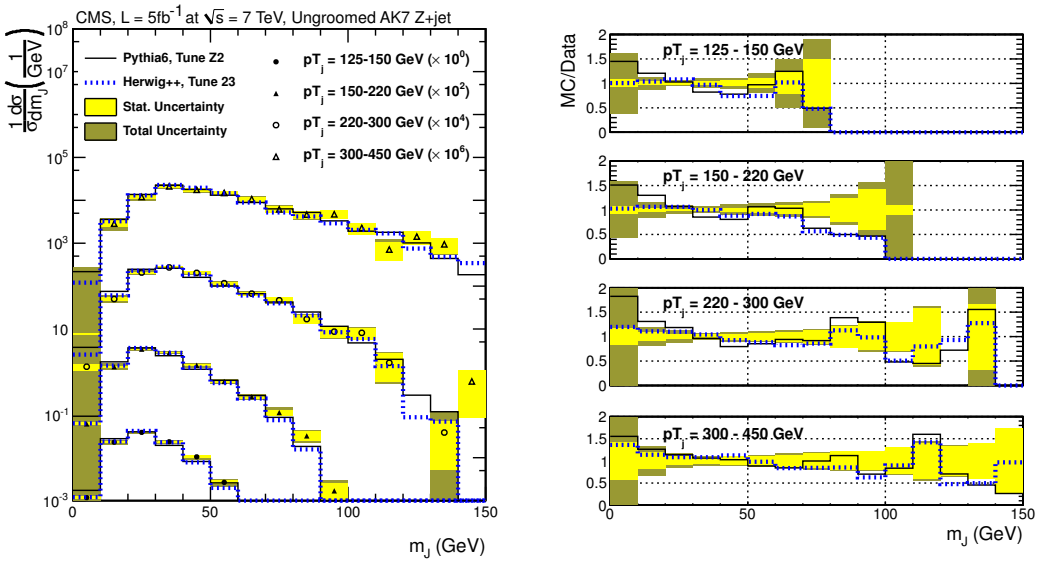

Figure 12. Unfolded, ungroomed AK7 m_J distribution for Z($\ell\ell$)+jet events. The data (black symbols) are compared to MC expectations from MadGraph+pythia6 (solid lines) and herwig++ (dotted lines) on the left. The ratio of MC to data is given on the right. The statistical uncertainty is shown in light shading, and the total uncertainty in dark shading.

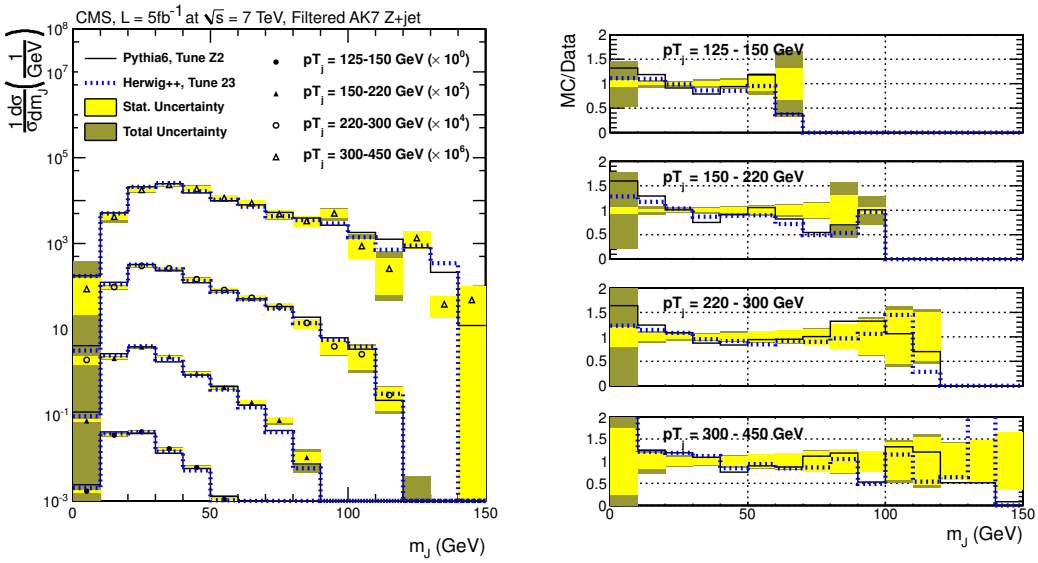

Figure 13. Unfolded AK7 filtered m_J distribution for Z($\ell\ell$)+jet events. The data (black symbols) are compared to MC expectations from MadGraph+pythia6 (solid lines) and herwig++ (dotted lines) on the left. The ratio of MC to data is given on the right. The statistical uncertainty is shown in light shading, and the total uncertainty in dark shading.

For clarity, the distributions are also truncated at large mass values where few events are recorded. Jet-mass bins with relative uncertainties $> 100\%$ are also ignored to minimize overlap with more precise measurements in other p_T bins.

Figures 12–15 show mass distributions for the leading AK7 jet accompanying a Z boson in Z($\ell\ell$)+jet events for the ungroomed, filtered, trimmed, and pruned clustering of jets,

JHEP05(2013)090

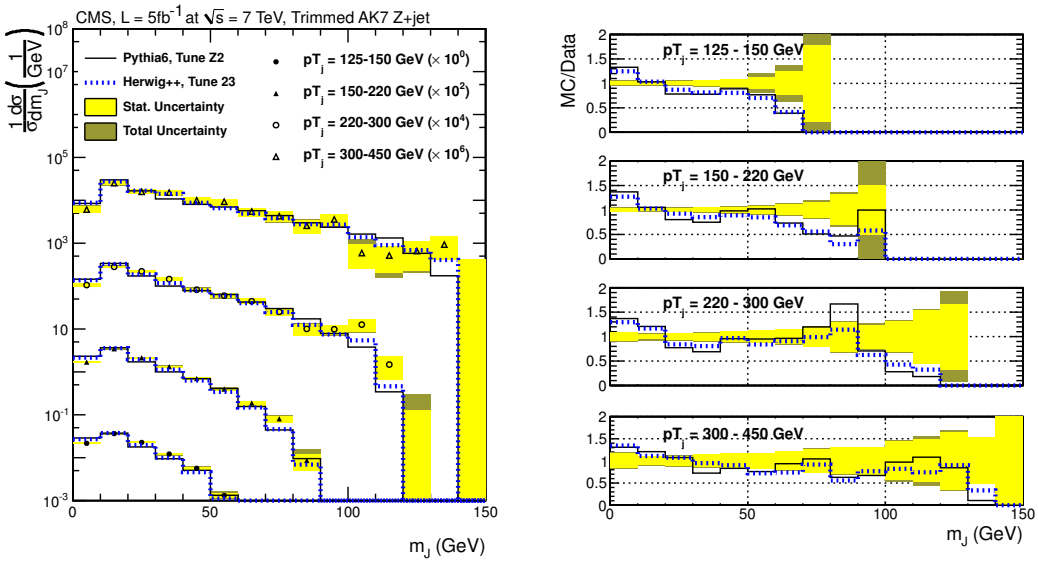

Figure 14. Unfolded AK7 trimmed m_J distribution for Z($\ell\ell$)+jet events. The data (black symbols) are compared to MC expectations from MadGraph+pythia6 (solid lines) and herwig++ (dotted lines) on the left. The ratio of MC to data is given on the right. The statistical uncertainty is shown in light shading, and the total uncertainty in dark shading.

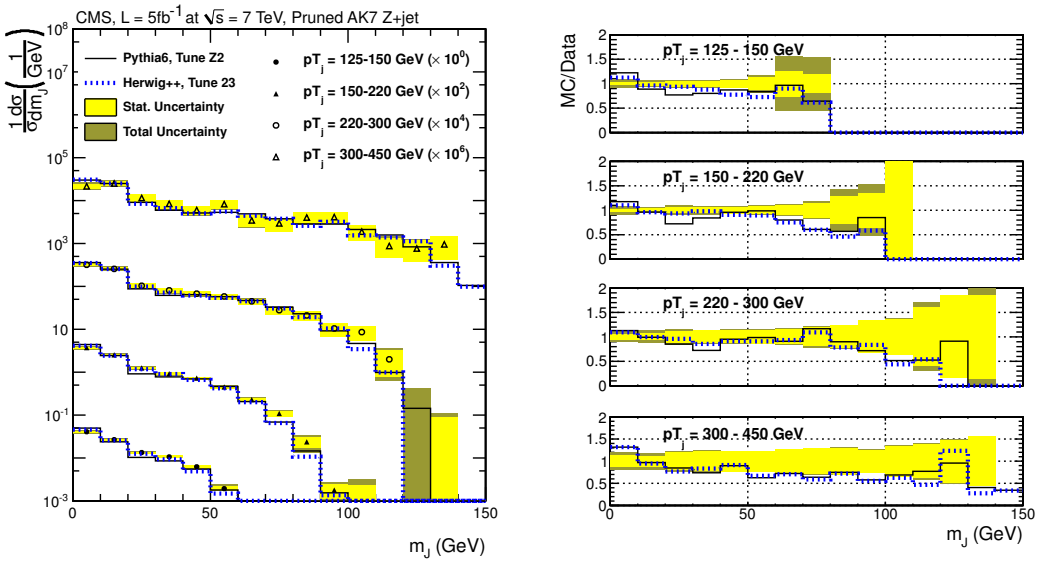

Figure 15. Unfolded AK7 pruned m_J distribution for Z($\ell\ell$)+jet events. The data (black symbols) are compared to MC expectations from MadGraph+pythia6 (solid lines) and herwig++ (dotted lines) on the left. The ratio of MC to data is given on the right. The statistical uncertainty is shown in light shading, and the total uncertainty in dark shading.

respectively. Both pythia6 and herwig++ show good agreement with data for all p_T bins, but especially so for $p_T > 300$ GeV. As in the case of the dijet analysis, the data at small jet mass are not modeled satisfactorily, but show modest improvement after applying the grooming procedures. To investigate several popular choices of jet grooming at CMS, figures 16–17 show the distributions in m_J for pruned CA8 and filtered CA12 jets in Z+jet

JHEP05(2013)090

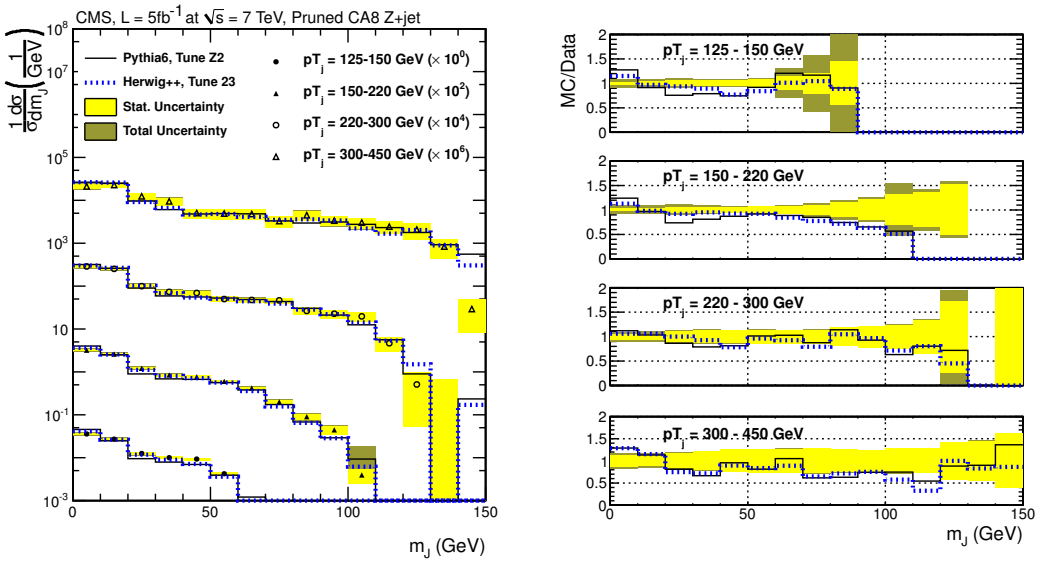

Figure 16. Unfolded CA8 pruned m_J distribution for Z($\ell\ell$)+jet events. The data (black symbols) are compared to MC expectations from MadGraph+pythia6 (solid lines) and herwig++ (dotted lines) on the left. The ratio of MC to data is given on the right. The statistical uncertainty is shown in light shading, and the total uncertainty in dark shading.

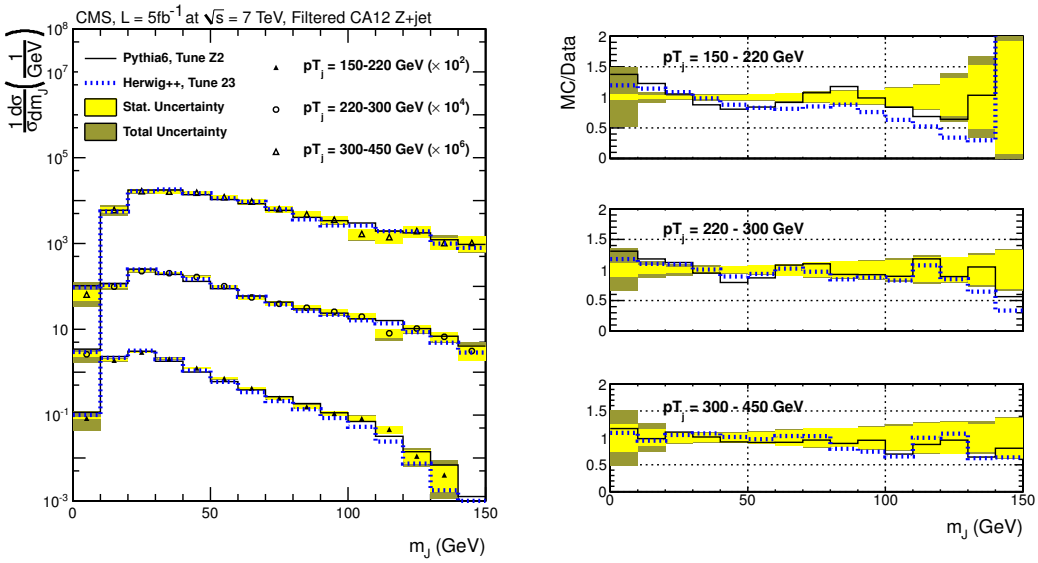

Figure 17. Unfolded CA12 filtered m_J distribution for Z($\ell\ell$)+jet events. The data (black symbols) are compared to MC expectations from MadGraph+pythia6 (solid lines) and herwig++ (dotted lines) on the left. The ratio of MC to data is given on the right. The statistical uncertainty is shown in light shading, and the total uncertainty in dark shading.

events. For groomed CA jets, both pythia6 and herwig++ provide good agreement with the data, with some possible inconsistency for $m_J < 20\,\text{GeV}$ and at large m_J for $p_T < 300\,\text{GeV}$ for the ungroomed and filtered jets. Figures 18–21 show the corresponding distributions for the mass of the leading jet accompanying the W boson for AK7 jets in

JHEP05(2013)090

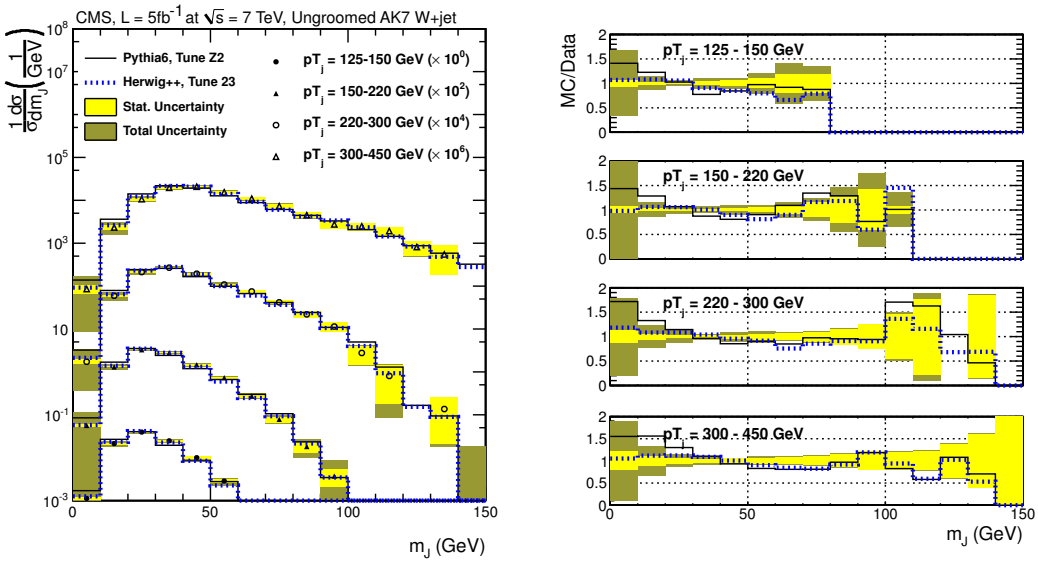

Figure 18. Distributions in m_J for unfolded, ungroomed AK7 jets in W($\ell\nu_\ell$)+jet events. The data (black symbols) are compared to MC expectations from MadGraph+pythia6 (solid lines) and herwig++ (dotted lines) on the left. The ratios of MC to data are given on the right. The statistical uncertainty is shown in light shading, and the total uncertainty in dark shading.

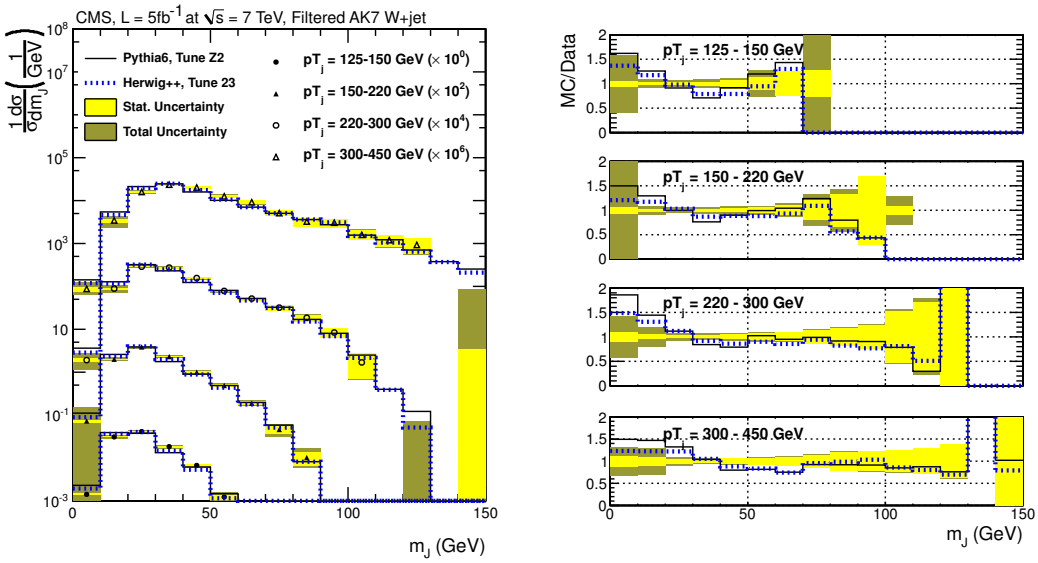

Figure 19. Distributions in m_J for unfolded, filtered AK7 jets in W($\ell\nu_\ell$)+jet events. The data (black symbols) for different bins in p_T are compared to MC expectations from MadGraph+pythia6 (solid lines) and herwig++ (dotted lines) on the left. The ratios of MC to data are given on the right. The statistical uncertainty is shown in light shading, and the total uncertainty in dark shading.

W($\ell\nu_\ell$)+jet events for the ungroomed, filtered, trimmed, and pruned clustering algorithms, and figures 22–23 show the distributions for pruned CA8 and filtered CA12 jets. For CA8 and CA12 jets, only particular grooming algorithms and p_T bins are chosen for illustration. The MC simulation shows good agreement with data, just as observed for Z+jet events.

JHEP05(2013)090

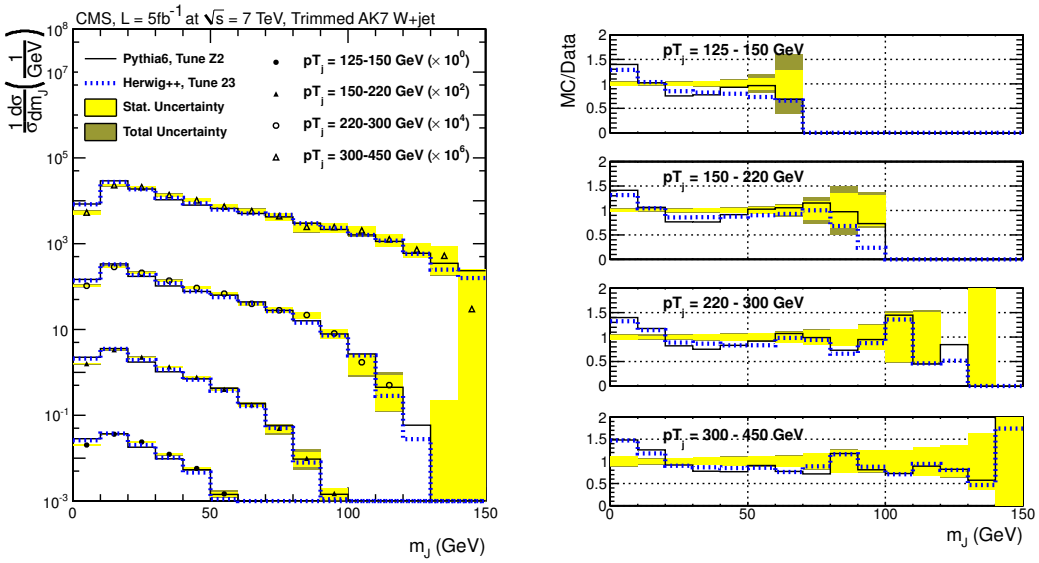

Figure 20. Distributions in m_J for unfolded, trimmed AK7 jets in W($\ell\nu_\ell$)+jet events. The data (black symbols) for different bins in p_T are compared to MC expectations from MadGraph+pythia6 (solid lines) and herwig++ (dotted lines) on the left. The ratios of MC to data are given on the right. The statistical uncertainty is shown in light shading, and the total uncertainty in dark shading.

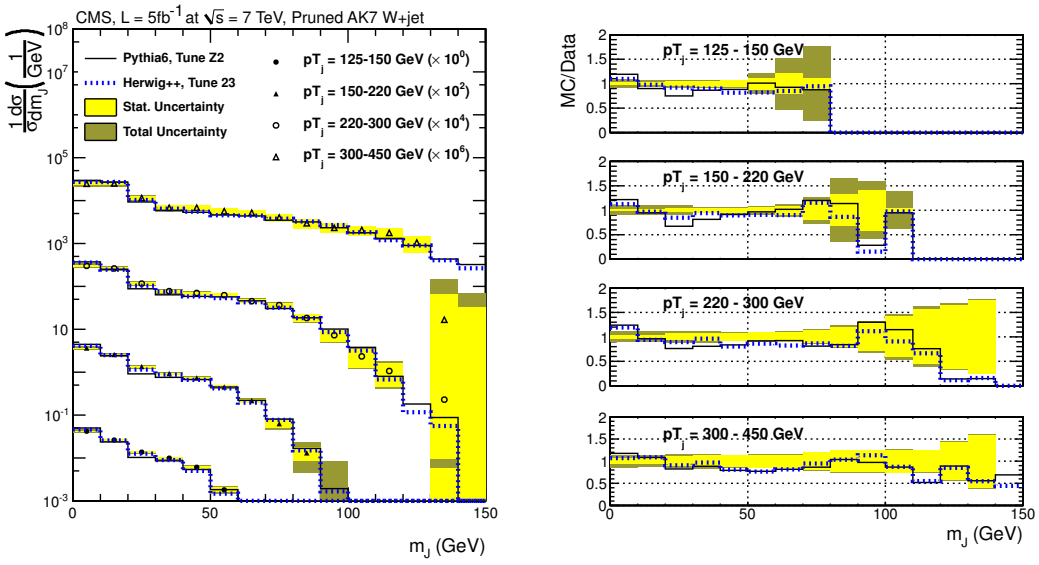

Figure 21. Distributions in m_J for unfolded, pruned AK7 jets in W($\ell\nu_\ell$)+jet events. The data (black symbols) for different bins in p_T are compared to MC expectations from MadGraph+pythia6 (solid lines) and herwig++ (dotted lines) on the left. The ratios of MC to data are given on the right. The statistical uncertainty is shown in light shading, and the total uncertainty in dark shading.

JHEP05(2013)090

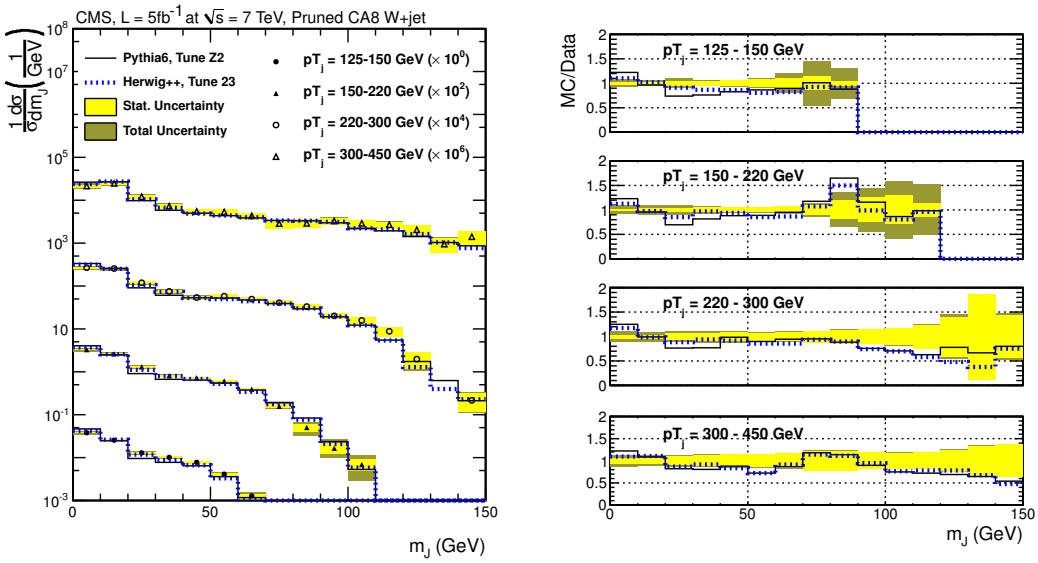

Figure 22. Distributions in m_J for unfolded, pruned CA8 jets in W($\ell\nu_\ell$)+jet events. The data (black symbols) for different bins in p_T are compared to MC expectations from MADGRAPH+PYTHIA6 (solid lines) and HERWIG++ (dotted lines) on the left. The ratios of MC to data are given on the right. The statistical uncertainty is shown in light shading, and the total uncertainty in dark shading.

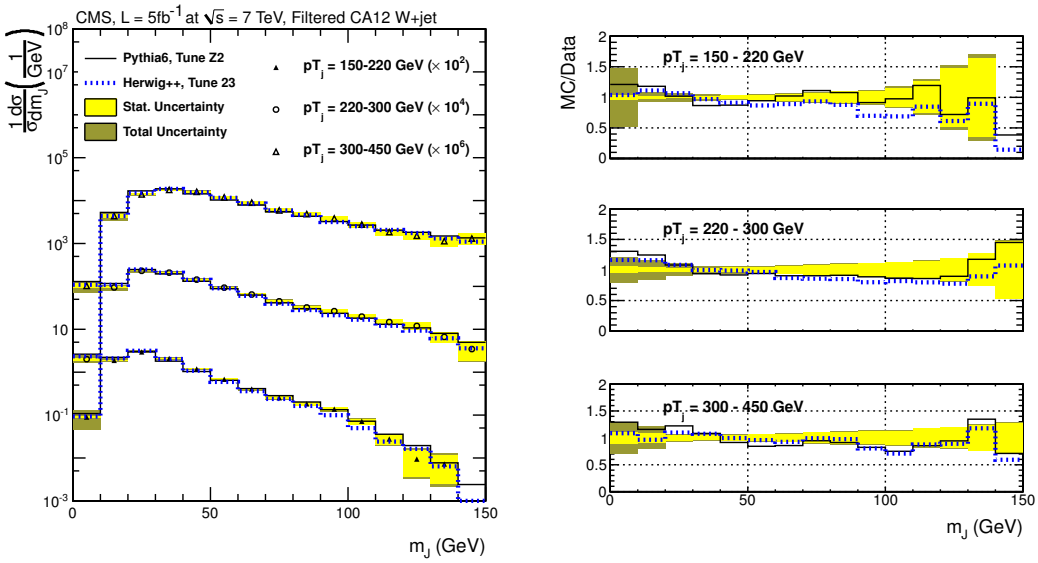

Figure 23. Distributions in m_J for unfolded, filtered CA12 jets in W($\ell\nu_\ell$)+jet events. The data (black symbols) for different bins in p_T are compared to MC expectations from MADGRAPH+PYTHIA6 (solid lines) and HERWIG++ (dotted lines) on the left. The ratios of MC to data are given on the right. The statistical uncertainty is shown in light shading, and the total uncertainty in dark shading.

JHEP05(2013)090

10 Summary

We have presented the differential distributions in jet mass for inclusive dijet and V+jet events, defined through the anti-k_{T} algorithm for a size parameter of 0.7 for ungroomed jets, as well as for jets groomed through filtering, trimming, and pruning. In addition, similar distributions for V+jet events were given for pruned Cambridge-Aachen jets with a size parameter of 0.8, as well as for filtered Cambridge-Aachen jets with a size parameter of 1.2. The impact of pileup on jet mass was also investigated.

Higher-order QCD matrix-element predictions for partons, coupled to parton-shower Monte Carlo programs that generate jet mass in dijet and V+jet events, are found to be in good agreement with data. A comparison of data with MC simulation indicates that both PYTHIA6 and HERWIG++ reproduce the data reasonably well, and that the HERWIG++ predictions for more aggressive grooming algorithms, i.e., those that remove larger fractions of contributions to the original ungroomed jet mass, agree somewhat better with observations. It is also observed that the more aggressive grooming procedures lead to somewhat better agreement between data and MC simulation.

In comparing the results from the V+jet analysis with those for the two leading jets in multijet events, the predictions provide slightly better agreement with the V+jet data. This observation suggests that simulation of quark jets is better than of gluon jets. Differences between data and simulation are larger at small jet mass values, which also correspond to the region more affected by pileup and soft QCD radiation.

These studies represent the first detailed investigations of techniques for characterizing jet substructure based on data collected by the CMS experiment at a center-of-mass energy of 7 TeV. For the trimming and pruning algorithms, these studies mark the first publication on this subject from the LHC, and provide an important benchmark for their use in searches for massive particles. Finally, the intrinsic stability of these algorithms to pileup effects is likely to contribute to a more rapid and widespread use of these techniques in future high-luminosity runs at the LHC.

Acknowledgments

We congratulate our colleagues in the CERN accelerator departments for the excellent performance of the LHC and thank the technical and administrative staffs at CERN and at other CMS institutes for their contributions to the success of the CMS effort. In addition, we gratefully acknowledge the computing centres and personnel of the Worldwide LHC Computing Grid for delivering so effectively the computing infrastructure essential to our analyses. Finally, we acknowledge the enduring support for the construction and operation of the LHC and the CMS detector provided by the following funding agencies: the Austrian Federal Ministry of Science and Research and the Austrian Science Fund; the Belgian Fonds de la Recherche Scientifique, and Fonds voor Wetenschappelijk Onderzoek; the Brazilian Funding Agencies (CNPq, CAPES, FAPERJ, and FAPESP); the Bulgarian Ministry of Education, Youth and Science; CERN; the Chinese Academy of Sciences, Ministry of Science and Technology, and National Natural Science Foundation of China; the

JHEP05(2013)090

Colombian Funding Agency (COLCIENCIAS); the Croatian Ministry of Science, Education and Sport; the Research Promotion Foundation, Cyprus; the Ministry of Education and Research, Recurrent financing contract SF0690030s09 and European Regional Development Fund, Estonia; the Academy of Finland, Finnish Ministry of Education and Culture, and Helsinki Institute of Physics; the Institut National de Physique Nucléaire et de Physique des Particules / CNRS, and Commissariat à l'Énergie Atomique et aux Énergies Alternatives / CEA, France; the Bundesministerium für Bildung und Forschung, Deutsche Forschungsgemeinschaft, and Helmholtz-Gemeinschaft Deutscher Forschungszentren, Germany; the General Secretariat for Research and Technology, Greece; the National Scientific Research Foundation, and National Office for Research and Technology, Hungary; the Department of Atomic Energy and the Department of Science and Technology, India; the Institute for Studies in Theoretical Physics and Mathematics, Iran; the Science Foundation, Ireland; the Istituto Nazionale di Fisica Nucleare, Italy; the Korean Ministry of Education, Science and Technology and the World Class University program of NRF, Republic of Korea; the Lithuanian Academy of Sciences; the Mexican Funding Agencies (CINVESTAV, CONACYT, SEP, and UASLP-FAI); the Ministry of Science and Innovation, New Zealand; the Pakistan Atomic Energy Commission; the Ministry of Science and Higher Education and the National Science Centre, Poland; the Fundação para a Ciência e a Tecnologia, Portugal; JINR (Armenia, Belarus, Georgia, Ukraine, Uzbekistan); the Ministry of Education and Science of the Russian Federation, the Federal Agency of Atomic Energy of the Russian Federation, Russian Academy of Sciences, and the Russian Foundation for Basic Research; the Ministry of Science and Technological Development of Serbia; the Secretaría de Estado de Investigación, Desarrollo e Innovación and Programa Consolider-Ingenio 2010, Spain; the Swiss Funding Agencies (ETH Board, ETH Zurich, PSI, SNF, UniZH, Canton Zurich, and SER); the National Science Council, Taipei; the Thailand Center of Excellence in Physics, the Institute for the Promotion of Teaching Science and Technology of Thailand and the National Science and Technology Development Agency of Thailand; the Scientific and Technical Research Council of Turkey, and Turkish Atomic Energy Authority; the Science and Technology Facilities Council, UK; the US Department of Energy, and the US National Science Foundation.

Individuals have received support from the Marie-Curie programme and the European Research Council and EPLANET (European Union); the Leventis Foundation; the A. P. Sloan Foundation; the Alexander von Humboldt Foundation; the Belgian Federal Science Policy Office; the Fonds pour la Formation à la Recherche dans l'Industrie et dans l'Agriculture (FRIA-Belgium); the Agentschap voor Innovatie door Wetenschap en Technologie (IWT-Belgium); the Ministry of Education, Youth and Sports (MEYS) of Czech Republic; the Council of Science and Industrial Research, India; the Compagnia di San Paolo (Torino); and the HOMING PLUS programme of Foundation for Polish Science, cofinanced from European Union, Regional Development Fund.

JHEP05(2013)090

References

[1] A. Abdesselam et al., *Boosted objects: a probe of beyond the standard model physics*, *Eur. Phys. J.* **C 71** (2011) 1661 [arXiv:1012.5412] [INSPIRE].

[2] CDF collaboration, T. Aaltonen et al., *Study of substructure of high transverse momentum jets produced in proton-antiproton collisions at* $\sqrt{s} = 1.96$ *TeV*, *Phys. Rev.* **D 85** (2012) 091101 [arXiv:1106.5952] [INSPIRE].

[3] ATLAS collaboration, *Jet mass and substructure of inclusive jets in* $\sqrt{s} = 7$ *TeV pp collisions with the ATLAS experiment*, *JHEP* **05** (2012) 128 [arXiv:1203.4606] [INSPIRE].

[4] K. Khelifa-Kerfa, *Non-global logs and clustering impact on jet mass with a jet veto distribution*, *JHEP* **02** (2012) 072 [arXiv:1111.2016] [INSPIRE].

[5] A. Hornig, C. Lee, J.R. Walsh and S. Zuberi, *Double non-global logarithms in-n-out of jets*, *JHEP* **01** (2012) 149 [arXiv:1110.0004] [INSPIRE].

[6] H.-n. Li, Z. Li and C.-P. Yuan, *QCD resummation for jet substructures*, *Phys. Rev. Lett.* **107** (2011) 152001 [arXiv:1107.4535] [INSPIRE].

[7] C.W. Bauer, F.J. Tackmann, J.R. Walsh and S. Zuberi, *Factorization and resummation for dijet invariant mass spectra*, *Phys. Rev.* **D 85** (2012) 074006 [arXiv:1106.6047] [INSPIRE].

[8] Y.-T. Chien and M.D. Schwartz, *Resummation of heavy jet mass and comparison to LEP data*, *JHEP* **08** (2010) 058 [arXiv:1005.1644] [INSPIRE].

[9] M.D. Schwartz, *Resummation and NLO matching of event shapes with effective field theory*, *Phys. Rev.* **D 77** (2008) 014026 [arXiv:0709.2709] [INSPIRE].

[10] S. Fleming, A.H. Hoang, S. Mantry and I.W. Stewart, *Jets from massive unstable particles: top-mass determination*, *Phys. Rev.* **D 77** (2008) 074010 [hep-ph/0703207] [INSPIRE].

[11] M. Dasgupta and G. Salam, *Resummation of nonglobal QCD observables*, *Phys. Lett.* **B 512** (2001) 323 [hep-ph/0104277] [INSPIRE].

[12] C.W. Bauer and M.D. Schwartz, *Event generation from effective field theory*, *Phys. Rev.* **D 76** (2007) 074004 [hep-ph/0607296] [INSPIRE].

[13] C.W. Bauer and M.D. Schwartz, *Improving jet distributions with effective field theory*, *Phys. Rev. Lett.* **97** (2006) 142001 [hep-ph/0604065] [INSPIRE].

[14] A. Hornig, C. Lee, I.W. Stewart, J.R. Walsh and S. Zuberi, *Non-global structure of the* $O(\alpha_s^2)$ *dijet soft function*, *JHEP* **08** (2011) 054 [arXiv:1105.4628] [INSPIRE].

[15] R. Kelley, M.D. Schwartz, R.M. Schabinger and H.X. Zhu, *The two-loop hemisphere soft function*, *Phys. Rev.* **D 84** (2011) 045022 [arXiv:1105.3676] [INSPIRE].

[16] T.T. Jouttenus, *Jet function with a jet algorithm in SCET*, *Phys. Rev.* **D 81** (2010) 094017 [arXiv:0912.5509] [INSPIRE].

[17] S.D. Ellis, A. Hornig, C. Lee, C.K. Vermilion and J.R. Walsh, *Consistent factorization of jet observables in exclusive multijet cross-sections*, *Phys. Lett.* **B 689** (2010) 82 [arXiv:0912.0262] [INSPIRE].

[18] S.D. Ellis, C.K. Vermilion, J.R. Walsh, A. Hornig and C. Lee, *Jet shapes and jet algorithms in SCET*, *JHEP* **11** (2010) 101 [arXiv:1001.0014] [INSPIRE].

[19] W. M.-Y. Cheung, M. Luke and S. Zuberi, *Phase space and jet definitions in SCET*, *Phys. Rev.* **D 80** (2009) 114021 [arXiv:0910.2479] [INSPIRE].

JHEP05(2013)090

[20] R. Kelley and M.D. Schwartz, *Threshold hadronic event shapes with effective field theory*, *Phys. Rev.* **D 83** (2011) 033001 [arXiv:1008.4355] [INSPIRE].

[21] A. Banfi, M. Dasgupta, K. Khelifa-Kerfa and S. Marzani, *Non-global logarithms and jet algorithms in high-pT jet shapes*, *JHEP* **08** (2010) 064 [arXiv:1004.3483] [INSPIRE].

[22] C.W. Bauer, D. Pirjol and I.W. Stewart, *Soft collinear factorization in effective field theory*, *Phys. Rev.* **D 65** (2002) 054022 [hep-ph/0109045] [INSPIRE].

[23] M. Dasgupta et al., *On jet mass distributions in Z + jet and dijet processes at the LHC*, *JHEP* **10** (2012) 126 [arXiv:1207.1640] [INSPIRE].

[24] J.M. Butterworth, A.R. Davison, M. Rubin and G.P. Salam, *Jet substructure as a new Higgs search channel at the LHC*, *Phys. Rev. Lett.* **100** (2008) 242001 [arXiv:0802.2470] [INSPIRE].

[25] D. Krohn, J. Thaler and L.-T. Wang, *Jet trimming*, *JHEP* **02** (2010) 084 [arXiv:0912.1342] [INSPIRE].

[26] S.D. Ellis, C.K. Vermilion and J.R. Walsh, *Techniques for improved heavy particle searches with jet substructure*, *Phys. Rev.* **D 80** (2009) 051501 [arXiv:0903.5081] [INSPIRE].

[27] S.D. Ellis, C.K. Vermilion and J.R. Walsh, *Recombination algorithms and jet substructure: pruning as a tool for heavy particle searches*, *Phys. Rev.* **D 81** (2010) 094023 [arXiv:0912.0033] [INSPIRE].

[28] M. Whalley and J. Bentham, *HEPDATA Project*, HEPDATA record for this paper is at http://hepdata.cedar.ac.uk/view/ins1224539.

[29] M. Cacciari, G.P. Salam and G. Soyez, *The anti-k_t jet clustering algorithm*, *JHEP* **04** (2008) 063 [arXiv:0802.1189] [INSPIRE].

[30] M. Cacciari, G.P. Salam and G. Soyez, *The catchment area of jets*, *JHEP* **04** (2008) 005 [arXiv:0802.1188] [INSPIRE].

[31] Y.L. Dokshitzer, G. Leder, S. Moretti and B. Webber, *Better jet clustering algorithms*, *JHEP* **08** (1997) 001 [hep-ph/9707323] [INSPIRE].

[32] M. Wobisch and T. Wengler, *Hadronization corrections to jet cross-sections in deep inelastic scattering*, hep-ph/9907280 [INSPIRE].

[33] J. Butterworth, B. Cox and J.R. Forshaw, *WW scattering at the CERN LHC*, *Phys. Rev.* **D 65** (2002) 096014 [hep-ph/0201098] [INSPIRE].

[34] CMS collaboration, *Search for anomalous $t\bar{t}$ production in the highly-boosted all-hadronic final state*, *JHEP* **09** (2012) 029 [arXiv:1204.2488] [INSPIRE].

[35] T. Sjöstrand et al., *High-energy physics event generation with PYTHIA 6.1*, *Comput. Phys. Commun.* **135** (2001) 238 [hep-ph/0010017] [INSPIRE].

[36] CMS collaboration, *The CMS experiment at the CERN LHC*, 2008 *JINST* **3** S08004 [INSPIRE].

[37] CMS collaboration, *Particle-flow event reconstruction in CMS and performance for jets, taus and MET*, CMS-PAS-PFT-09-001 (2009).

[38] R. Field, *Early LHC underlying event data — Findings and surprises*, arXiv:1010.3558 [INSPIRE].

JHEP05(2013)090

[39] T. Sjöstrand, S. Mrenna and P.Z. Skands, *A brief introduction to PYTHIA 8.1*, *Comput. Phys. Commun.* **178** (2008) 852 [arXiv:0710.3820] [INSPIRE].

[40] M. Bähr et al., *HERWIG++ physics and Manual*, *Eur. Phys. J.* **C 58** (2008) 639 [arXiv:0803.0883] [INSPIRE].

[41] J. Allison et al., *Geant4: developments and applications*, *IEEE Trans. Nucl. Sci.* **53** (2006) 270 [INSPIRE].

[42] J. Alwall, M. Herquet, F. Maltoni, O. Mattelaer and T. Stelzer, *MadGraph 5: going beyond*, *JHEP* **06** (2011) 128 [arXiv:1106.0522] [INSPIRE].

[43] S. Frixione, P. Nason and C. Oleari, *Matching NLO QCD computations with Parton Shower simulations: the POWHEG method*, *JHEP* **11** (2007) 070 [arXiv:0709.2092] [INSPIRE].

[44] J. Pumplin et al., *New generation of parton distributions with uncertainties from global QCD analysis*, *JHEP* **07** (2002) 012 [hep-ph/0201195] [INSPIRE].

[45] M. Cacciari and G.P. Salam, *Dispelling the N^3 myth for the k_t jet-finder*, *Phys. Lett.* **B 641** (2006) 57 [hep-ph/0512210] [INSPIRE].

[46] M. Cacciari, G.P. Salam and G. Soyez, *FastJet user manual*, *Eur. Phys. J.* **C 72** (2012) 1896 [arXiv:1111.6097] [INSPIRE].

[47] CMS collaboration, *Electron reconstruction and identification at $\sqrt{s} = 7$ TeV*, CMS-PAS-EGM-10-004 (2010).

[48] CMS collaboration, *Performance of CMS muon reconstruction in pp collision events at $\sqrt{s} = 7$ TeV*, 2012 *JINST* **7** P10002 [arXiv:1206.4071] [INSPIRE].

[49] M. Cacciari and G.P. Salam, *Pileup subtraction using jet areas*, *Phys. Lett.* **B 659** (2008) 119 [arXiv:0707.1378] [INSPIRE].

[50] CMS collaboration, *Determination of jet energy calibration and transverse momentum resolution in CMS*, 2011 *JINST* **6** P11002 [arXiv:1107.4277] [INSPIRE].

[51] M. Dasgupta, L. Magnea and G.P. Salam, *Non-perturbative QCD effects in jets at hadron colliders*, *JHEP* **02** (2008) 055 [arXiv:0712.3014] [INSPIRE].

[52] L.B. Lucy, *An iterative technique for the rectification of observed distributions*, *Astron. J.* **79** (1974) 745.

[53] W.H. Richardson, *Bayesian-based iterative method of image restoration*, *J. Opt. Soc. Am.* **62** (1972) 55.

[54] L.A. Shepp and Y. Vardi, *Maximum likelihood reconstruction for emission tomography*, *IEEE Trans. Med. Imag.* **1** (1982) 113.

[55] Y. Vardi, L. Shepp and L. Kaufman, *A statistical model for positron emission tomography*, *J. Am. Stat. Assoc.* **80** (1985) 8.

[56] G. D'Agostini, *A multidimensional unfolding method based on Bayes' theorem*, *Nucl. Instrum. Meth.* **A 362** (1995) 487 [INSPIRE].

JHEP05(2013)090

The CMS collaboration

Yerevan Physics Institute, Yerevan, Armenia

S. Chatrchyan, V. Khachatryan, A.M. Sirunyan, A. Tumasyan

Institut für Hochenergiephysik der OeAW, Wien, Austria

W. Adam, E. Aguilo, T. Bergauer, M. Dragicevic, J. Erö, C. Fabjan[1], M. Friedl, R. Frühwirth[1], V.M. Ghete, N. Hörmann, J. Hrubec, M. Jeitler[1], W. Kiesenhofer, V. Knünz, M. Krammer[1], I. Krätschmer, D. Liko, I. Mikulec, M. Pernicka†, D. Rabady[2], B. Rahbaran, C. Rohringer, H. Rohringer, R. Schöfbeck, J. Strauss, A. Taurok, W. Waltenberger, C.-E. Wulz[1]

National Centre for Particle and High Energy Physics, Minsk, Belarus

V. Mossolov, N. Shumeiko, J. Suarez Gonzalez

Universiteit Antwerpen, Antwerpen, Belgium

S. Alderweireldt, M. Bansal, S. Bansal, T. Cornelis, E.A. De Wolf, X. Janssen, S. Luyckx, L. Mucibello, S. Ochesanu, B. Roland, R. Rougny, H. Van Haevermaet, P. Van Mechelen, N. Van Remortel, A. Van Spilbeeck

Vrije Universiteit Brussel, Brussel, Belgium

F. Blekman, S. Blyweert, J. D'Hondt, R. Gonzalez Suarez, A. Kalogeropoulos, M. Maes, A. Olbrechts, S. Tavernier, W. Van Doninck, P. Van Mulders, G.P. Van Onsem, I. Villella

Université Libre de Bruxelles, Bruxelles, Belgium

B. Clerbaux, G. De Lentdecker, V. Dero, A.P.R. Gay, T. Hreus, A. Léonard, P.E. Marage, A. Mohammadi, T. Reis, L. Thomas, C. Vander Velde, P. Vanlaer, J. Wang

Ghent University, Ghent, Belgium

V. Adler, K. Beernaert, A. Cimmino, S. Costantini, G. Garcia, M. Grunewald, B. Klein, J. Lellouch, A. Marinov, J. Mccartin, A.A. Ocampo Rios, D. Ryckbosch, M. Sigamani, N. Strobbe, F. Thyssen, M. Tytgat, S. Walsh, E. Yazgan, N. Zaganidis

Université Catholique de Louvain, Louvain-la-Neuve, Belgium

S. Basegmez, G. Bruno, R. Castello, L. Ceard, C. Delaere, T. du Pree, D. Favart, L. Forthomme, A. Giammanco[3], J. Hollar, V. Lemaitre, J. Liao, O. Militaru, C. Nuttens, D. Pagano, A. Pin, K. Piotrzkowski, M. Selvaggi, J.M. Vizan Garcia

Université de Mons, Mons, Belgium

N. Beliy, T. Caebergs, E. Daubie, G.H. Hammad

Centro Brasileiro de Pesquisas Fisicas, Rio de Janeiro, Brazil

G.A. Alves, M. Correa Martins Junior, T. Martins, M.E. Pol, M.H.G. Souza

Universidade do Estado do Rio de Janeiro, Rio de Janeiro, Brazil

W.L. Aldá Júnior, W. Carvalho, J. Chinellato, A. Custódio, E.M. Da Costa, D. De Jesus Damiao, C. De Oliveira Martins, S. Fonseca De Souza, H. Malbouisson, M. Malek, D. Matos Figueiredo, L. Mundim, H. Nogima, W.L. Prado Da Silva, A. Santoro, L. Soares Jorge, A. Sznajder, E.J. Tonelli Manganote, A. Vilela Pereira

JHEP05(2013)090

Universidade Estadual Paulista [a], Universidade Federal do ABC [b], São Paulo, Brazil

T.S. Anjos[b], C.A. Bernardes[b], F.A. Dias[a,4], T.R. Fernandez Perez Tomei[a], E.M. Gregores[b], C. Lagana[a], F. Marinho[a], P.G. Mercadante[b], S.F. Novaes[a], Sandra S. Padula[a]

Institute for Nuclear Research and Nuclear Energy, Sofia, Bulgaria

V. Genchev[2], P. Iaydjiev[2], S. Piperov, M. Rodozov, S. Stoykova, G. Sultanov, V. Tcholakov, R. Trayanov, M. Vutova

University of Sofia, Sofia, Bulgaria

A. Dimitrov, R. Hadjiiska, V. Kozhuharov, L. Litov, B. Pavlov, P. Petkov

Institute of High Energy Physics, Beijing, China

J.G. Bian, G.M. Chen, H.S. Chen, C.H. Jiang, D. Liang, S. Liang, X. Meng, J. Tao, J. Wang, X. Wang, Z. Wang, H. Xiao, M. Xu, J. Zang, Z. Zhang

State Key Laboratory of Nuclear Physics and Technology, Peking University, Beijing, China

C. Asawatangtrakuldee, Y. Ban, Y. Guo, Q. Li, W. Li, S. Liu, Y. Mao, S.J. Qian, D. Wang, L. Zhang, W. Zou

Universidad de Los Andes, Bogota, Colombia

C. Avila, C.A. Carrillo Montoya, J.P. Gomez, B. Gomez Moreno, A.F. Osorio Oliveros, J.C. Sanabria

Technical University of Split, Split, Croatia

N. Godinovic, D. Lelas, R. Plestina[5], D. Polic, I. Puljak[2]

University of Split, Split, Croatia

Z. Antunovic, M. Kovac

Institute Rudjer Boskovic, Zagreb, Croatia

V. Brigljevic, S. Duric, K. Kadija, J. Luetic, D. Mekterovic, S. Morovic, L. Tikvica

University of Cyprus, Nicosia, Cyprus

A. Attikis, M. Galanti, G. Mavromanolakis, J. Mousa, C. Nicolaou, F. Ptochos, P.A. Razis

Charles University, Prague, Czech Republic

M. Finger, M. Finger Jr.

Academy of Scientific Research and Technology of the Arab Republic of Egypt, Egyptian Network of High Energy Physics, Cairo, Egypt

Y. Assran[6], S. Elgammal[7], A. Ellithi Kamel[8], M.A. Mahmoud[9], A. Radi[10,11]

National Institute of Chemical Physics and Biophysics, Tallinn, Estonia

M. Kadastik, M. Müntel, M. Murumaa, M. Raidal, L. Rebane, A. Tiko

Department of Physics, University of Helsinki, Helsinki, Finland

P. Eerola, G. Fedi, M. Voutilainen

JHEP05(2013)090

Helsinki Institute of Physics, Helsinki, Finland

J. Härkönen, A. Heikkinen, V. Karimäki, R. Kinnunen, M.J. Kortelainen, T. Lampén, K. Lassila-Perini, S. Lehti, T. Lindén, P. Luukka, T. Mäenpää, T. Peltola, E. Tuominen, J. Tuominiemi, E. Tuovinen, D. Ungaro, L. Wendland

Lappeenranta University of Technology, Lappeenranta, Finland

A. Korpela, T. Tuuva

DSM/IRFU, CEA/Saclay, Gif-sur-Yvette, France

M. Besancon, S. Choudhury, F. Couderc, M. Dejardin, D. Denegri, B. Fabbro, J.L. Faure, F. Ferri, S. Ganjour, A. Givernaud, P. Gras, G. Hamel de Monchenault, P. Jarry, E. Locci, J. Malcles, L. Millischer, A. Nayak, J. Rander, A. Rosowsky, M. Titov

Laboratoire Leprince-Ringuet, Ecole Polytechnique, IN2P3-CNRS, Palaiseau, France

S. Baffioni, F. Beaudette, L. Benhabib, L. Bianchini, M. Bluj[12], P. Busson, C. Charlot, N. Daci, T. Dahms, M. Dalchenko, L. Dobrzynski, A. Florent, R. Granier de Cassagnac, M. Haguenauer, P. Miné, C. Mironov, I.N. Naranjo, M. Nguyen, C. Ochando, P. Paganini, D. Sabes, R. Salerno, Y. Sirois, C. Veelken, A. Zabi

Institut Pluridisciplinaire Hubert Curien, Université de Strasbourg, Université de Haute Alsace Mulhouse, CNRS/IN2P3, Strasbourg, France

J.-L. Agram[13], J. Andrea, D. Bloch, D. Bodin, J.-M. Brom, M. Cardaci, E.C. Chabert, C. Collard, E. Conte[13], F. Drouhin[13], J.-C. Fontaine[13], D. Gelé, U. Goerlach, P. Juillot, A.-C. Le Bihan, P. Van Hove

Université de Lyon, Université Claude Bernard Lyon 1, CNRS-IN2P3, Institut de Physique Nucléaire de Lyon, Villeurbanne, France

S. Beauceron, N. Beaupere, O. Bondu, G. Boudoul, S. Brochet, J. Chasserat, R. Chierici[2], D. Contardo, P. Depasse, H. El Mamouni, J. Fay, S. Gascon, M. Gouzevitch, B. Ille, T. Kurca, M. Lethuillier, L. Mirabito, S. Perries, L. Sgandurra, V. Sordini, Y. Tschudi, P. Verdier, S. Viret

Institute of High Energy Physics and Informatization, Tbilisi State University, Tbilisi, Georgia

Z. Tsamalaidze[14]

RWTH Aachen University, I. Physikalisches Institut, Aachen, Germany

C. Autermann, S. Beranek, B. Calpas, M. Edelhoff, L. Feld, N. Heracleous, O. Hindrichs, R. Jussen, K. Klein, J. Merz, A. Ostapchuk, A. Perieanu, F. Raupach, J. Sammet, S. Schael, D. Sprenger, H. Weber, B. Wittmer, V. Zhukov[15]

RWTH Aachen University, III. Physikalisches Institut A, Aachen, Germany

M. Ata, J. Caudron, E. Dietz-Laursonn, D. Duchardt, M. Erdmann, R. Fischer, A. Güth, T. Hebbeker, C. Heidemann, K. Hoepfner, D. Klingebiel, P. Kreuzer, M. Merschmeyer, A. Meyer, M. Olschewski, K. Padeken, P. Papacz, H. Pieta, H. Reithler, S.A. Schmitz, L. Sonnenschein, J. Steggemann, D. Teyssier, S. Thüer, M. Weber

JHEP05(2013)090

RWTH Aachen University, III. Physikalisches Institut B, Aachen, Germany

M. Bontenackels, V. Cherepanov, Y. Erdogan, G. Flügge, H. Geenen, M. Geisler, W. Haj Ahmad, F. Hoehle, B. Kargoll, T. Kress, Y. Kuessel, J. Lingemann[2], A. Nowack, I.M. Nugent, L. Perchalla, O. Pooth, P. Sauerland, A. Stahl

Deutsches Elektronen-Synchrotron, Hamburg, Germany

M. Aldaya Martin, I. Asin, N. Bartosik, J. Behr, W. Behrenhoff, U. Behrens, M. Bergholz[16], A. Bethani, K. Borras, A. Burgmeier, A. Cakir, L. Calligaris, A. Campbell, E. Castro, F. Costanza, D. Dammann, C. Diez Pardos, T. Dorland, G. Eckerlin, D. Eckstein, G. Flucke, A. Geiser, I. Glushkov, P. Gunnellini, S. Habib, J. Hauk, G. Hellwig, H. Jung, M. Kasemann, P. Katsas, C. Kleinwort, H. Kluge, A. Knutsson, M. Krämer, D. Krücker, E. Kuznetsova, W. Lange, J. Leonard, W. Lohmann[16], B. Lutz, R. Mankel, I. Marfin, M. Marienfeld, I.-A. Melzer-Pellmann, A.B. Meyer, J. Mnich, A. Mussgiller, S. Naumann-Emme, O. Novgorodova, F. Nowak, J. Olzem, H. Perrey, A. Petrukhin, D. Pitzl, A. Raspereza, P.M. Ribeiro Cipriano, C. Riedl, E. Ron, M. Rosin, J. Salfeld-Nebgen, R. Schmidt[16], T. Schoerner-Sadenius, N. Sen, A. Spiridonov, M. Stein, R. Walsh, C. Wissing

University of Hamburg, Hamburg, Germany

V. Blobel, H. Enderle, J. Erfle, U. Gebbert, M. Görner, M. Gosselink, J. Haller, T. Hermanns, R.S. Höing, K. Kaschube, G. Kaussen, H. Kirschenmann, R. Klanner, J. Lange, T. Peiffer, N. Pietsch, D. Rathjens, C. Sander, H. Schettler, P. Schleper, E. Schlieckau, A. Schmidt, M. Schröder, T. Schum, M. Seidel, J. Sibille[17], V. Sola, H. Stadie, G. Steinbrück, J. Thomsen, L. Vanelderen

Institut für Experimentelle Kernphysik, Karlsruhe, Germany

C. Barth, C. Baus, J. Berger, C. Böser, T. Chwalek, W. De Boer, A. Descroix, A. Dierlamm, M. Feindt, M. Guthoff[2], C. Hackstein, F. Hartmann[2], T. Hauth[2], M. Heinrich, H. Held, K.H. Hoffmann, U. Husemann, I. Katkov[15], J.R. Komaragiri, P. Lobelle Pardo, D. Martschei, S. Mueller, Th. Müller, M. Niegel, A. Nürnberg, O. Oberst, A. Oehler, J. Ott, G. Quast, K. Rabbertz, F. Ratnikov, N. Ratnikova, S. Röcker, F.-P. Schilling, G. Schott, H.J. Simonis, F.M. Stober, D. Troendle, R. Ulrich, J. Wagner-Kuhr, S. Wayand, T. Weiler, M. Zeise

Institute of Nuclear and Particle Physics (INPP), NCSR Demokritos, Aghia Paraskevi, Greece

G. Anagnostou, G. Daskalakis, T. Geralis, S. Kesisoglou, A. Kyriakis, D. Loukas, I. Manolakos, A. Markou, C. Markou, E. Ntomari

University of Athens, Athens, Greece

L. Gouskos, T.J. Mertzimekis, A. Panagiotou, N. Saoulidou

University of Ioánnina, Ioánnina, Greece

I. Evangelou, C. Foudas, P. Kokkas, N. Manthos, I. Papadopoulos

JHEP05(2013)090

KFKI Research Institute for Particle and Nuclear Physics, Budapest, Hungary
G. Bencze, C. Hajdu, P. Hidas, D. Horvath[18], F. Sikler, V. Veszpremi, G. Vesztergombi[19], A.J. Zsigmond

Institute of Nuclear Research ATOMKI, Debrecen, Hungary
N. Beni, S. Czellar, J. Molnar, J. Palinkas, Z. Szillasi

University of Debrecen, Debrecen, Hungary
J. Karancsi, P. Raics, Z.L. Trocsanyi, B. Ujvari

Panjab University, Chandigarh, India
S.B. Beri, V. Bhatnagar, N. Dhingra, R. Gupta, M. Kaur, M.Z. Mehta, M. Mittal, N. Nishu, L.K. Saini, A. Sharma, J.B. Singh

University of Delhi, Delhi, India
Ashok Kumar, Arun Kumar, S. Ahuja, A. Bhardwaj, B.C. Choudhary, S. Malhotra, M. Naimuddin, K. Ranjan, P. Saxena, V. Sharma, R.K. Shivpuri

Saha Institute of Nuclear Physics, Kolkata, India
S. Banerjee, S. Bhattacharya, K. Chatterjee, S. Dutta, B. Gomber, Sa. Jain, Sh. Jain, R. Khurana, A. Modak, S. Mukherjee, D. Roy, S. Sarkar, M. Sharan

Bhabha Atomic Research Centre, Mumbai, India
A. Abdulsalam, D. Dutta, S. Kailas, V. Kumar, A.K. Mohanty[2], L.M. Pant, P. Shukla

Tata Institute of Fundamental Research - EHEP, Mumbai, India
T. Aziz, R.M. Chatterjee, S. Ganguly, M. Guchait[20], A. Gurtu[21], M. Maity[22], G. Majumder, K. Mazumdar, G.B. Mohanty, B. Parida, K. Sudhakar, N. Wickramage

Tata Institute of Fundamental Research - HECR, Mumbai, India
S. Banerjee, S. Dugad

Institute for Research in Fundamental Sciences (IPM), Tehran, Iran
H. Arfaei[23], H. Bakhshiansohi, S.M. Etesami[24], A. Fahim[23], M. Hashemi[25], H. Hesari, A. Jafari, M. Khakzad, M. Mohammadi Najafabadi, S. Paktinat Mehdiabadi, B. Safarzadeh[26], M. Zeinali

INFN Sezione di Bari [a], Università di Bari [b], Politecnico di Bari [c], Bari, Italy
M. Abbrescia[a,b], L. Barbone[a,b], C. Calabria[a,b,2], S.S. Chhibra[a,b], A. Colaleo[a], D. Creanza[a,c], N. De Filippis[a,c,2], M. De Palma[a,b], L. Fiore[a], G. Iaselli[a,c], G. Maggi[a,c], M. Maggi[a], B. Marangelli[a,b], S. My[a,c], S. Nuzzo[a,b], N. Pacifico[a], A. Pompili[a,b], G. Pugliese[a,c], G. Selvaggi[a,b], L. Silvestris[a], G. Singh[a,b], R. Venditti[a,b], P. Verwilligen[a], G. Zito[a]

INFN Sezione di Bologna [a], Università di Bologna [b], Bologna, Italy
G. Abbiendi[a], A.C. Benvenuti[a], D. Bonacorsi[a,b], S. Braibant-Giacomelli[a,b], L. Brigliadori[a,b], P. Capiluppi[a,b], A. Castro[a,b], F.R. Cavallo[a], M. Cuffiani[a,b], G.M. Dallavalle[a], F. Fabbri[a], A. Fanfani[a,b], D. Fasanella[a,b], P. Giacomelli[a], C. Grandi[a], L. Guiducci[a,b], S. Marcellini[a], G. Masetti[a], M. Meneghelli[a,b,2], A. Montanari[a],

JHEP05(2013)090

F.L. Navarria[a,b], F. Odorici[a], A. Perrotta[a], F. Primavera[a,b], A.M. Rossi[a,b], T. Rovelli[a,b], G.P. Siroli[a,b], N. Tosi[a,b], R. Travaglini[a,b]

INFN Sezione di Catania [a], Università di Catania [b], Catania, Italy

S. Albergo[a,b], G. Cappello[a,b], M. Chiorboli[a,b], S. Costa[a,b], R. Potenza[a,b], A. Tricomi[a,b], C. Tuve[a,b]

INFN Sezione di Firenze [a], Università di Firenze [b], Firenze, Italy

G. Barbagli[a], V. Ciulli[a,b], C. Civinini[a], R. D'Alessandro[a,b], E. Focardi[a,b], S. Frosali[a,b], E. Gallo[a], S. Gonzi[a,b], M. Meschini[a], S. Paoletti[a], G. Sguazzoni[a], A. Tropiano[a,b]

INFN Laboratori Nazionali di Frascati, Frascati, Italy

L. Benussi, S. Bianco, S. Colafranceschi[27], F. Fabbri, D. Piccolo

INFN Sezione di Genova [a], Università di Genova [b], Genova, Italy

P. Fabbricatore[a], R. Musenich[a], S. Tosi[a,b]

INFN Sezione di Milano-Bicocca [a], Università di Milano-Bicocca [b], Milano, Italy

A. Benaglia[a], F. De Guio[a,b], L. Di Matteo[a,b,2], S. Fiorendi[a,b], S. Gennai[a,2], A. Ghezzi[a,b], M.T. Lucchini[2], S. Malvezzi[a], R.A. Manzoni[a,b], A. Martelli[a,b], A. Massironi[a,b], D. Menasce[a], L. Moroni[a], M. Paganoni[a,b], D. Pedrini[a], S. Ragazzi[a,b], N. Redaelli[a], T. Tabarelli de Fatis[a,b]

INFN Sezione di Napoli [a], Università di Napoli 'Federico II' [b], Università della Basilicata (Potenza) [c], Università G. Marconi (Roma) [d], Napoli, Italy

S. Buontempo[a], N. Cavallo[a,c], A. De Cosa[a,b,2], O. Dogangun[a,b], F. Fabozzi[a,c], A.O.M. Iorio[a,b], L. Lista[a], S. Meola[a,d,28], M. Merola[a], P. Paolucci[a,2]

INFN Sezione di Padova [a], Università di Padova [b], Università di Trento (Trento) [c], Padova, Italy

P. Azzi[a], N. Bacchetta[a,2], A. Branca[a,b,2], R. Carlin[a,b], P. Checchia[a], T. Dorigo[a], F. Gasparini[a,b], U. Gasparini[a,b], A. Gozzelino[a], K. Kanishchev[a,c], S. Lacaprara[a], I. Lazzizzera[a,c], M. Margoni[a,b], A.T. Meneguzzo[a,b], J. Pazzini[a,b], N. Pozzobon[a,b], P. Ronchese[a,b], M. Sgaravatto[a], F. Simonetto[a,b], E. Torassa[a], M. Tosi[a,b], S. Vanini[a,b], P. Zotto[a,b], A. Zucchetta[a,b], G. Zumerle[a,b]

INFN Sezione di Pavia [a], Università di Pavia [b], Pavia, Italy

M. Gabusi[a,b], S.P. Ratti[a,b], C. Riccardi[a,b], P. Torre[a,b], P. Vitulo[a,b]

INFN Sezione di Perugia [a], Università di Perugia [b], Perugia, Italy

M. Biasini[a,b], G.M. Bilei[a], L. Fanò[a,b], P. Lariccia[a,b], G. Mantovani[a,b], M. Menichelli[a], A. Nappi[a,b†], F. Romeo[a,b], A. Saha[a], A. Santocchia[a,b], A. Spiezia[a,b], S. Taroni[a,b]

INFN Sezione di Pisa [a], Università di Pisa [b], Scuola Normale Superiore di Pisa [c], Pisa, Italy

P. Azzurri[a,c], G. Bagliesi[a], J. Bernardini[a], T. Boccali[a], G. Broccolo[a,c], R. Castaldi[a], R.T. D'Agnolo[a,c,2], R. Dell'Orso[a], F. Fiori[a,b,2], L. Foà[a,c], A. Giassi[a], A. Kraan[a],

JHEP05(2013)090

F. Ligabue[a,c], T. Lomtadze[a], L. Martini[a,29], A. Messineo[a,b], F. Palla[a], A. Rizzi[a,b], A.T. Serban[a,30], P. Spagnolo[a], P. Squillacioti[a,2], R. Tenchini[a], G. Tonelli[a,b], A. Venturi[a], P.G. Verdini[a]

INFN Sezione di Roma [a], Università di Roma [b], Roma, Italy

L. Barone[a,b], F. Cavallari[a], D. Del Re[a,b], M. Diemoz[a], C. Fanelli[a,b], M. Grassi[a,b,2], E. Longo[a,b], P. Meridiani[a,2], F. Micheli[a,b], S. Nourbakhsh[a,b], G. Organtini[a,b], R. Paramatti[a], S. Rahatlou[a,b], L. Soffi[a,b]

INFN Sezione di Torino [a], Università di Torino [b], Università del Piemonte Orientale (Novara) [c], Torino, Italy

N. Amapane[a,b], R. Arcidiacono[a,c], S. Argiro[a,b], M. Arneodo[a,c], C. Biino[a], N. Cartiglia[a], S. Casasso[a,b], M. Costa[a,b], N. Demaria[a], C. Mariotti[a,2], S. Maselli[a], E. Migliore[a,b], V. Monaco[a,b], M. Musich[a,2], M.M. Obertino[a,c], N. Pastrone[a], M. Pelliccioni[a], A. Potenza[a,b], A. Romero[a,b], M. Ruspa[a,c], R. Sacchi[a,b], A. Solano[a,b], A. Staiano[a]

INFN Sezione di Trieste [a], Università di Trieste [b], Trieste, Italy

S. Belforte[a], V. Candelise[a,b], M. Casarsa[a], F. Cossutti[a,2], G. Della Ricca[a,b], B. Gobbo[a], M. Marone[a,b,2], D. Montanino[a,b], A. Penzo[a], A. Schizzi[a,b]

Kangwon National University, Chunchon, Korea

T.Y. Kim, S.K. Nam

Kyungpook National University, Daegu, Korea

S. Chang, D.H. Kim, G.N. Kim, D.J. Kong, H. Park, D.C. Son

Chonnam National University, Institute for Universe and Elementary Particles, Kwangju, Korea

J.Y. Kim, Zero J. Kim, S. Song

Korea University, Seoul, Korea

S. Choi, D. Gyun, B. Hong, M. Jo, H. Kim, T.J. Kim, K.S. Lee, D.H. Moon, S.K. Park, Y. Roh

University of Seoul, Seoul, Korea

M. Choi, J.H. Kim, C. Park, I.C. Park, S. Park, G. Ryu

Sungkyunkwan University, Suwon, Korea

Y. Choi, Y.K. Choi, J. Goh, M.S. Kim, E. Kwon, B. Lee, J. Lee, S. Lee, H. Seo, I. Yu

Vilnius University, Vilnius, Lithuania

M.J. Bilinskas, I. Grigelionis, M. Janulis, A. Juodagalvis

Centro de Investigacion y de Estudios Avanzados del IPN, Mexico City, Mexico

H. Castilla-Valdez, E. De La Cruz-Burelo, I. Heredia-de La Cruz, R. Lopez-Fernandez, J. Martínez-Ortega, A. Sanchez-Hernandez, L.M. Villasenor-Cendejas

Universidad Iberoamericana, Mexico City, Mexico

S. Carrillo Moreno, F. Vazquez Valencia

JHEP05(2013)090

Benemerita Universidad Autonoma de Puebla, Puebla, Mexico
H.A. Salazar Ibarguen

Universidad Autónoma de San Luis Potosí, San Luis Potosí, Mexico
E. Casimiro Linares, A. Morelos Pineda, M.A. Reyes-Santos

University of Auckland, Auckland, New Zealand
D. Krofcheck

University of Canterbury, Christchurch, New Zealand
A.J. Bell, P.H. Butler, R. Doesburg, S. Reucroft, H. Silverwood

National Centre for Physics, Quaid-I-Azam University, Islamabad, Pakistan
M. Ahmad, M.I. Asghar, J. Butt, H.R. Hoorani, S. Khalid, W.A. Khan, T. Khurshid, S. Qazi, M.A. Shah, M. Shoaib

National Centre for Nuclear Research, Swierk, Poland
H. Bialkowska, B. Boimska, T. Frueboes, M. Górski, M. Kazana, K. Nawrocki, K. Romanowska-Rybinska, M. Szleper, G. Wrochna, P. Zalewski

Institute of Experimental Physics, Faculty of Physics, University of Warsaw, Warsaw, Poland
G. Brona, K. Bunkowski, M. Cwiok, W. Dominik, K. Doroba, A. Kalinowski, M. Konecki, J. Krolikowski, M. Misiura, W. Wolszczak

Laboratório de Instrumentação e Física Experimental de Partículas, Lisboa, Portugal
N. Almeida, P. Bargassa, A. David, P. Faccioli, P.G. Ferreira Parracho, M. Gallinaro, J. Seixas, J. Varela, P. Vischia

Joint Institute for Nuclear Research, Dubna, Russia
P. Bunin, I. Golutvin, I. Gorbunov, A. Kamenev, V. Karjavin, V. Konoplyanikov, G. Kozlov, A. Lanev, A. Malakhov, P. Moisenz, V. Palichik, V. Perelygin, S. Shmatov, S. Shulha, V. Smirnov, A. Volodko, A. Zarubin

Petersburg Nuclear Physics Institute, Gatchina (St. Petersburg), Russia
S. Evstyukhin, V. Golovtsov, Y. Ivanov, V. Kim, P. Levchenko, V. Murzin, V. Oreshkin, I. Smirnov, V. Sulimov, L. Uvarov, S. Vavilov, A. Vorobyev, An. Vorobyev

Institute for Nuclear Research, Moscow, Russia
Yu. Andreev, A. Dermenev, S. Gninenko, N. Golubev, M. Kirsanov, N. Krasnikov, V. Matveev, A. Pashenkov, D. Tlisov, A. Toropin

Institute for Theoretical and Experimental Physics, Moscow, Russia
V. Epshteyn, M. Erofeeva, V. Gavrilov, M. Kossov, N. Lychkovskaya, V. Popov, G. Safronov, S. Semenov, I. Shreyber, V. Stolin, E. Vlasov, A. Zhokin

P.N. Lebedev Physical Institute, Moscow, Russia
V. Andreev, M. Azarkin, I. Dremin, M. Kirakosyan, A. Leonidov, G. Mesyats, S.V. Rusakov, A. Vinogradov

JHEP05(2013)090

Skobeltsyn Institute of Nuclear Physics, Lomonosov Moscow State University, Moscow, Russia

A. Belyaev, E. Boos, M. Dubinin[4], L. Dudko, A. Ershov, A. Gribushin, V. Klyukhin, O. Kodolova, I. Lokhtin, A. Markina, S. Obraztsov, M. Perfilov, S. Petrushanko, A. Popov, L. Sarycheva[†], V. Savrin, A. Snigirev

State Research Center of Russian Federation, Institute for High Energy Physics, Protvino, Russia

I. Azhgirey, I. Bayshev, S. Bitioukov, V. Grishin[2], V. Kachanov, D. Konstantinov, V. Krychkine, V. Petrov, R. Ryutin, A. Sobol, L. Tourtchanovitch, S. Troshin, N. Tyurin, A. Uzunian, A. Volkov

University of Belgrade, Faculty of Physics and Vinca Institute of Nuclear Sciences, Belgrade, Serbia

P. Adzic[31], M. Djordjevic, M. Ekmedzic, D. Krpic[31], J. Milosevic

Centro de Investigaciones Energéticas Medioambientales y Tecnológicas (CIEMAT), Madrid, Spain

M. Aguilar-Benitez, J. Alcaraz Maestre, P. Arce, C. Battilana, E. Calvo, M. Cerrada, M. Chamizo Llatas, N. Colino, B. De La Cruz, A. Delgado Peris, D. Domínguez Vázquez, C. Fernandez Bedoya, J.P. Fernández Ramos, A. Ferrando, J. Flix, M.C. Fouz, P. Garcia-Abia, O. Gonzalez Lopez, S. Goy Lopez, J.M. Hernandez, M.I. Josa, G. Merino, J. Puerta Pelayo, A. Quintario Olmeda, I. Redondo, L. Romero, J. Santaolalla, M.S. Soares, C. Willmott

Universidad Autónoma de Madrid, Madrid, Spain

C. Albajar, G. Codispoti, J.F. de Trocóniz

Universidad de Oviedo, Oviedo, Spain

H. Brun, J. Cuevas, J. Fernandez Menendez, S. Folgueras, I. Gonzalez Caballero, L. Lloret Iglesias, J. Piedra Gomez

Instituto de Física de Cantabria (IFCA), CSIC-Universidad de Cantabria, Santander, Spain

J.A. Brochero Cifuentes, I.J. Cabrillo, A. Calderon, S.H. Chuang, J. Duarte Campderros, M. Felcini[32], M. Fernandez, G. Gomez, J. Gonzalez Sanchez, A. Graziano, C. Jorda, A. Lopez Virto, J. Marco, R. Marco, C. Martinez Rivero, F. Matorras, F.J. Munoz Sanchez, T. Rodrigo, A.Y. Rodríguez-Marrero, A. Ruiz-Jimeno, L. Scodellaro, I. Vila, R. Vilar Cortabitarte

CERN, European Organization for Nuclear Research, Geneva, Switzerland

D. Abbaneo, E. Auffray, G. Auzinger, M. Bachtis, P. Baillon, A.H. Ball, D. Barney, J.F. Benitez, C. Bernet[5], G. Bianchi, P. Bloch, A. Bocci, A. Bonato, C. Botta, H. Breuker, T. Camporesi, G. Cerminara, T. Christiansen, J.A. Coarasa Perez, D. D'Enterria, A. Dabrowski, A. De Roeck, S. De Visscher, S. Di Guida, M. Dobson, N. Dupont-Sagorin, A. Elliott-Peisert, B. Frisch, W. Funk, G. Georgiou, M. Giffels, D. Gigi, K. Gill, D. Giordano, M. Girone, M. Giunta, F. Glege, R. Gomez-Reino Garrido, P. Govoni,

JHEP05(2013)090

S. Gowdy, R. Guida, J. Hammer, M. Hansen, P. Harris, C. Hartl, J. Harvey, B. Hegner, A. Hinzmann, V. Innocente, P. Janot, K. Kaadze, E. Karavakis, K. Kousouris, P. Lecoq, Y.-J. Lee, P. Lenzi, C. Lourenço, N. Magini, T. Mäki, M. Malberti, L. Malgeri, M. Mannelli, L. Masetti, F. Meijers, S. Mersi, E. Meschi, R. Moser, M. Mulders, P. Musella, E. Nesvold, L. Orsini, E. Palencia Cortezon, E. Perez, L. Perrozzi, A. Petrilli, A. Pfeiffer, M. Pierini, M. Pimiä, D. Piparo, G. Polese, L. Quertenmont, A. Racz, W. Reece, J. Rodrigues Antunes, G. Rolandi[33], C. Rovelli[34], M. Rovere, H. Sakulin, F. Santanastasio, C. Schäfer, C. Schwick, I. Segoni, S. Sekmen, A. Sharma, P. Siegrist, P. Silva, M. Simon, P. Sphicas[35], D. Spiga, A. Tsirou, G.I. Veres[19], J.R. Vlimant, H.K. Wöhri, S.D. Worm[36], W.D. Zeuner

Paul Scherrer Institut, Villigen, Switzerland

W. Bertl, K. Deiters, W. Erdmann, K. Gabathuler, R. Horisberger, Q. Ingram, H.C. Kaestli, S. König, D. Kotlinski, U. Langenegger, F. Meier, D. Renker, T. Rohe

Institute for Particle Physics, ETH Zurich, Zurich, Switzerland

F. Bachmair, L. Bäni, P. Bortignon, M.A. Buchmann, B. Casal, N. Chanon, A. Deisher, G. Dissertori, M. Dittmar, M. Donegà, M. Dünser, P. Eller, J. Eugster, K. Freudenreich, C. Grab, D. Hits, P. Lecomte, W. Lustermann, A.C. Marini, P. Martinez Ruiz del Arbol, N. Mohr, F. Moortgat, C. Nägeli[37], P. Nef, F. Nessi-Tedaldi, F. Pandolfi, L. Pape, F. Pauss, M. Peruzzi, F.J. Ronga, M. Rossini, L. Sala, A.K. Sanchez, A. Starodumov[38], B. Stieger, M. Takahashi, L. Tauscher†, A. Thea, K. Theofilatos, D. Treille, C. Urscheler, R. Wallny, H.A. Weber, L. Wehrli

Universität Zürich, Zurich, Switzerland

C. Amsler[39], V. Chiochia, C. Favaro, M. Ivova Rikova, B. Kilminster, B. Millan Mejias, P. Otiougova, P. Robmann, H. Snoek, S. Tupputi, M. Verzetti

National Central University, Chung-Li, Taiwan

Y.H. Chang, K.H. Chen, C. Ferro, C.M. Kuo, S.W. Li, W. Lin, Y.J. Lu, A.P. Singh, R. Volpe, S.S. Yu

National Taiwan University (NTU), Taipei, Taiwan

P. Bartalini, P. Chang, Y.H. Chang, Y.W. Chang, Y. Chao, K.F. Chen, C. Dietz, U. Grundler, W.-S. Hou, Y. Hsiung, K.Y. Kao, Y.J. Lei, R.-S. Lu, D. Majumder, E. Petrakou, X. Shi, J.G. Shiu, Y.M. Tzeng, X. Wan, M. Wang

Chulalongkorn University, Bangkok, Thailand

B. Asavapibhop, E. Simili, N. Srimanobhas, N. Suwonjandee

Cukurova University, Adana, Turkey

A. Adiguzel, M.N. Bakirci[40], S. Cerci[41], C. Dozen, I. Dumanoglu, E. Eskut, S. Girgis, G. Gokbulut, E. Gurpinar, I. Hos, E.E. Kangal, T. Karaman, G. Karapinar[42], A. Kayis Topaksu, G. Onengut, K. Ozdemir, S. Ozturk[43], A. Polatoz, K. Sogut[44], D. Sunar Cerci[41], B. Tali[41], H. Topakli[40], L.N. Vergili, M. Vergili

Middle East Technical University, Physics Department, Ankara, Turkey

I.V. Akin, T. Aliev, B. Bilin, S. Bilmis, M. Deniz, H. Gamsizkan, A.M. Guler, K. Ocalan, A. Ozpineci, M. Serin, R. Sever, U.E. Surat, M. Yalvac, E. Yildirim, M. Zeyrek

JHEP05(2013)090

Bogazici University, Istanbul, Turkey

E. Gülmez, B. Isildak[45], M. Kaya[46], O. Kaya[46], S. Ozkorucuklu[47], N. Sonmez[48]

Istanbul Technical University, Istanbul, Turkey

H. Bahtiyar[49], E. Barlas, K. Cankocak, Y.O. Günaydin[50], F.I. Vardarlı, M. Yücel

National Scientific Center, Kharkov Institute of Physics and Technology, Kharkov, Ukraine

L. Levchuk

University of Bristol, Bristol, United Kingdom

J.J. Brooke, E. Clement, D. Cussans, H. Flacher, R. Frazier, J. Goldstein, M. Grimes, G.P. Heath, H.F. Heath, L. Kreczko, S. Metson, D.M. Newbold[36], K. Nirunpong, A. Poll, S. Senkin, V.J. Smith, T. Williams

Rutherford Appleton Laboratory, Didcot, United Kingdom

L. Basso[51], K.W. Bell, A. Belyaev[51], C. Brew, R.M. Brown, D.J.A. Cockerill, J.A. Coughlan, K. Harder, S. Harper, J. Jackson, B.W. Kennedy, E. Olaiya, D. Petyt, B.C. Radburn-Smith, C.H. Shepherd-Themistocleous, I.R. Tomalin, W.J. Womersley

Imperial College, London, United Kingdom

R. Bainbridge, G. Ball, R. Beuselinck, O. Buchmuller, D. Colling, N. Cripps, M. Cutajar, P. Dauncey, G. Davies, M. Della Negra, W. Ferguson, J. Fulcher, D. Futyan, A. Gilbert, A. Guneratne Bryer, G. Hall, Z. Hatherell, J. Hays, G. Iles, M. Jarvis, G. Karapostoli, M. Kenzie, L. Lyons, A.-M. Magnan, J. Marrouche, B. Mathias, R. Nandi, J. Nash, A. Nikitenko[38], J. Pela, M. Pesaresi, K. Petridis, M. Pioppi[52], D.M. Raymond, S. Rogerson, A. Rose, C. Seez, P. Sharp[†], A. Sparrow, M. Stoye, A. Tapper, M. Vazquez Acosta, T. Virdee, S. Wakefield, N. Wardle, T. Whyntie

Brunel University, Uxbridge, United Kingdom

M. Chadwick, J.E. Cole, P.R. Hobson, A. Khan, P. Kyberd, D. Leggat, D. Leslie, W. Martin, I.D. Reid, P. Symonds, L. Teodorescu, M. Turner

Baylor University, Waco, USA

K. Hatakeyama, H. Liu, T. Scarborough

The University of Alabama, Tuscaloosa, USA

O. Charaf, S.I. Cooper, C. Henderson, P. Rumerio

Boston University, Boston, USA

A. Avetisyan, T. Bose, C. Fantasia, A. Heister, P. Lawson, D. Lazic, J. Rohlf, D. Sperka, J. St. John, L. Sulak

Brown University, Providence, USA

J. Alimena, S. Bhattacharya, G. Christopher, D. Cutts, Z. Demiragli, A. Ferapontov, A. Garabedian, U. Heintz, S. Jabeen, G. Kukartsev, E. Laird, G. Landsberg, M. Luk, M. Narain, M. Segala, T. Sinthuprasith, T. Speer

JHEP05(2013)090

University of California, Davis, Davis, USA

R. Breedon, G. Breto, M. Calderon De La Barca Sanchez, M. Caulfield, S. Chauhan, M. Chertok, J. Conway, R. Conway, P.T. Cox, J. Dolen, R. Erbacher, M. Gardner, R. Houtz, W. Ko, A. Kopecky, R. Lander, O. Mall, T. Miceli, R. Nelson, D. Pellett, F. Ricci-Tam, B. Rutherford, M. Searle, J. Smith, M. Squires, M. Tripathi, R. Vasquez Sierra, R. Yohay

University of California, Los Angeles, USA

V. Andreev, D. Cline, R. Cousins, J. Duris, S. Erhan, P. Everaerts, C. Farrell, J. Hauser, M. Ignatenko, C. Jarvis, G. Rakness, P. Schlein†, P. Traczyk, V. Valuev, M. Weber

University of California, Riverside, Riverside, USA

J. Babb, R. Clare, M.E. Dinardo, J. Ellison, J.W. Gary, F. Giordano, G. Hanson, H. Liu, O.R. Long, A. Luthra, H. Nguyen, S. Paramesvaran, J. Sturdy, S. Sumowidagdo, R. Wilken, S. Wimpenny

University of California, San Diego, La Jolla, USA

W. Andrews, J.G. Branson, G.B. Cerati, S. Cittolin, D. Evans, A. Holzner, R. Kelley, M. Lebourgeois, J. Letts, I. Macneill, B. Mangano, S. Padhi, C. Palmer, G. Petrucciani, M. Pieri, M. Sani, V. Sharma, S. Simon, E. Sudano, M. Tadel, Y. Tu, A. Vartak, S. Wasserbaech[53], F. Würthwein, A. Yagil, J. Yoo

University of California, Santa Barbara, Santa Barbara, USA

D. Barge, R. Bellan, C. Campagnari, M. D'Alfonso, T. Danielson, K. Flowers, P. Geffert, C. George, F. Golf, J. Incandela, C. Justus, P. Kalavase, D. Kovalskyi, V. Krutelyov, S. Lowette, R. Magaña Villalba, N. Mccoll, V. Pavlunin, J. Ribnik, J. Richman, R. Rossin, D. Stuart, W. To, C. West

California Institute of Technology, Pasadena, USA

A. Apresyan, A. Bornheim, J. Bunn, Y. Chen, E. Di Marco, J. Duarte, M. Gataullin, D. Kcira, Y. Ma, A. Mott, H.B. Newman, C. Rogan, M. Spiropulu, V. Timciuc, J. Veverka, R. Wilkinson, S. Xie, Y. Yang, R.Y. Zhu

Carnegie Mellon University, Pittsburgh, USA

V. Azzolini, A. Calamba, R. Carroll, T. Ferguson, Y. Iiyama, D.W. Jang, Y.F. Liu, M. Paulini, H. Vogel, I. Vorobiev

University of Colorado at Boulder, Boulder, USA

J.P. Cumalat, B.R. Drell, W.T. Ford, A. Gaz, E. Luiggi Lopez, J.G. Smith, K. Stenson, K.A. Ulmer, S.R. Wagner

Cornell University, Ithaca, USA

J. Alexander, A. Chatterjee, N. Eggert, L.K. Gibbons, B. Heltsley, W. Hopkins, A. Khukhunaishvili, B. Kreis, N. Mirman, G. Nicolas Kaufman, J.R. Patterson, A. Ryd, E. Salvati, W. Sun, W.D. Teo, J. Thom, J. Thompson, J. Tucker, Y. Weng, L. Winstrom, P. Wittich

Fairfield University, Fairfield, USA

D. Winn

JHEP05(2013)090

Fermi National Accelerator Laboratory, Batavia, USA

S. Abdullin, M. Albrow, J. Anderson, G. Apollinari, L.A.T. Bauerdick, A. Beretvas, J. Berryhill, P.C. Bhat, K. Burkett, J.N. Butler, V. Chetluru, H.W.K. Cheung, F. Chlebana, S. Cihangir, V.D. Elvira, I. Fisk, J. Freeman, Y. Gao, D. Green, O. Gutsche, J. Hanlon, R.M. Harris, J. Hirschauer, B. Hooberman, S. Jindariani, M. Johnson, U. Joshi, B. Klima, S. Kunori, S. Kwan, C. Leonidopoulos[54], J. Linacre, D. Lincoln, R. Lipton, J. Lykken, K. Maeshima, J.M. Marraffino, V.I. Martinez Outschoorn, S. Maruyama, D. Mason, P. McBride, K. Mishra, S. Mrenna, Y. Musienko[55], C. Newman-Holmes, V. O'Dell, E. Sexton-Kennedy, S. Sharma, W.J. Spalding, L. Spiegel, L. Taylor, S. Tkaczyk, N.V. Tran, L. Uplegger, E.W. Vaandering, R. Vidal, J. Whitmore, W. Wu, F. Yang, J.C. Yun

University of Florida, Gainesville, USA

D. Acosta, P. Avery, D. Bourilkov, M. Chen, T. Cheng, S. Das, M. De Gruttola, G.P. Di Giovanni, D. Dobur, A. Drozdetskiy, R.D. Field, M. Fisher, Y. Fu, I.K. Furic, J. Gartner, J. Hugon, B. Kim, J. Konigsberg, A. Korytov, A. Kropivnitskaya, T. Kypreos, J.F. Low, K. Matchev, P. Milenovic[56], G. Mitselmakher, L. Muniz, M. Park, R. Remington, A. Rinkevicius, P. Sellers, N. Skhirtladze, M. Snowball, J. Yelton, M. Zakaria

Florida International University, Miami, USA

V. Gaultney, S. Hewamanage, L.M. Lebolo, S. Linn, P. Markowitz, G. Martinez, J.L. Rodriguez

Florida State University, Tallahassee, USA

T. Adams, A. Askew, J. Bochenek, J. Chen, B. Diamond, S.V. Gleyzer, J. Haas, S. Hagopian, V. Hagopian, M. Jenkins, K.F. Johnson, H. Prosper, V. Veeraraghavan, M. Weinberg

Florida Institute of Technology, Melbourne, USA

M.M. Baarmand, B. Dorney, M. Hohlmann, H. Kalakhety, I. Vodopiyanov, F. Yumiceva

University of Illinois at Chicago (UIC), Chicago, USA

M.R. Adams, L. Apanasevich, Y. Bai, V.E. Bazterra, R.R. Betts, I. Bucinskaite, J. Callner, R. Cavanaugh, O. Evdokimov, L. Gauthier, C.E. Gerber, D.J. Hofman, S. Khalatyan, F. Lacroix, C. O'Brien, C. Silkworth, D. Strom, P. Turner, N. Varelas

The University of Iowa, Iowa City, USA

U. Akgun, E.A. Albayrak, B. Bilki[57], W. Clarida, F. Duru, S. Griffiths, J.-P. Merlo, H. Mermerkaya[58], A. Mestvirishvili, A. Moeller, J. Nachtman, C.R. Newsom, E. Norbeck, Y. Onel, F. Ozok[49], S. Sen, P. Tan, E. Tiras, J. Wetzel, T. Yetkin[59], K. Yi

Johns Hopkins University, Baltimore, USA

B.A. Barnett, B. Blumenfeld, S. Bolognesi, D. Fehling, G. Giurgiu, A.V. Gritsan, G. Hu, P. Maksimovic, M. Swartz, A. Whitbeck

The University of Kansas, Lawrence, USA

P. Baringer, A. Bean, G. Benelli, R.P. Kenny Iii, M. Murray, D. Noonan, S. Sanders, R. Stringer, G. Tinti, J.S. Wood

JHEP05(2013)090

Kansas State University, Manhattan, USA

A.F. Barfuss, T. Bolton, I. Chakaberia, A. Ivanov, S. Khalil, M. Makouski, Y. Maravin, S. Shrestha, I. Svintradze

Lawrence Livermore National Laboratory, Livermore, USA

J. Gronberg, D. Lange, F. Rebassoo, D. Wright

University of Maryland, College Park, USA

A. Baden, B. Calvert, S.C. Eno, J.A. Gomez, N.J. Hadley, R.G. Kellogg, M. Kirn, T. Kolberg, Y. Lu, M. Marionneau, A.C. Mignerey, K. Pedro, A. Peterman, A. Skuja, J. Temple, M.B. Tonjes, S.C. Tonwar

Massachusetts Institute of Technology, Cambridge, USA

A. Apyan, G. Bauer, J. Bendavid, W. Busza, E. Butz, I.A. Cali, M. Chan, V. Dutta, G. Gomez Ceballos, M. Goncharov, Y. Kim, M. Klute, K. Krajczar[60], A. Levin, P.D. Luckey, T. Ma, S. Nahn, C. Paus, D. Ralph, C. Roland, G. Roland, M. Rudolph, G.S.F. Stephans, F. Stöckli, K. Sumorok, K. Sung, D. Velicanu, E.A. Wenger, R. Wolf, B. Wyslouch, M. Yang, Y. Yilmaz, A.S. Yoon, M. Zanetti, V. Zhukova

University of Minnesota, Minneapolis, USA

B. Dahmes, A. De Benedetti, G. Franzoni, A. Gude, J. Haupt, S.C. Kao, K. Klapoetke, Y. Kubota, J. Mans, N. Pastika, R. Rusack, M. Sasseville, A. Singovsky, N. Tambe, J. Turkewitz

University of Mississippi, Oxford, USA

L.M. Cremaldi, R. Kroeger, L. Perera, R. Rahmat, D.A. Sanders

University of Nebraska-Lincoln, Lincoln, USA

E. Avdeeva, K. Bloom, S. Bose, D.R. Claes, A. Dominguez, M. Eads, J. Keller, I. Kravchenko, J. Lazo-Flores, S. Malik, G.R. Snow

State University of New York at Buffalo, Buffalo, USA

A. Godshalk, I. Iashvili, S. Jain, A. Kharchilava, A. Kumar, S. Rappoccio, Z. Wan

Northeastern University, Boston, USA

G. Alverson, E. Barberis, D. Baumgartel, M. Chasco, J. Haley, D. Nash, T. Orimoto, D. Trocino, D. Wood, J. Zhang

Northwestern University, Evanston, USA

A. Anastassov, K.A. Hahn, A. Kubik, L. Lusito, N. Mucia, N. Odell, R.A. Ofierzynski, B. Pollack, A. Pozdnyakov, M. Schmitt, S. Stoynev, M. Velasco, S. Won

University of Notre Dame, Notre Dame, USA

D. Berry, A. Brinkerhoff, K.M. Chan, M. Hildreth, C. Jessop, D.J. Karmgard, J. Kolb, K. Lannon, W. Luo, S. Lynch, N. Marinelli, D.M. Morse, T. Pearson, M. Planer, R. Ruchti, J. Slaunwhite, N. Valls, M. Wayne, M. Wolf

JHEP05(2013)090

The Ohio State University, Columbus, USA

L. Antonelli, B. Bylsma, L.S. Durkin, C. Hill, R. Hughes, K. Kotov, T.Y. Ling, D. Puigh, M. Rodenburg, C. Vuosalo, G. Williams, B.L. Winer

Princeton University, Princeton, USA

E. Berry, P. Elmer, V. Halyo, P. Hebda, J. Hegeman, A. Hunt, P. Jindal, S.A. Koay, D. Lopes Pegna, P. Lujan, D. Marlow, T. Medvedeva, M. Mooney, J. Olsen, P. Piroué, X. Quan, A. Raval, H. Saka, D. Stickland, C. Tully, J.S. Werner, S.C. Zenz, A. Zuranski

University of Puerto Rico, Mayaguez, USA

E. Brownson, A. Lopez, H. Mendez, J.E. Ramirez Vargas

Purdue University, West Lafayette, USA

E. Alagoz, V.E. Barnes, D. Benedetti, G. Bolla, D. Bortoletto, M. De Mattia, A. Everett, Z. Hu, M. Jones, O. Koybasi, M. Kress, A.T. Laasanen, N. Leonardo, V. Maroussov, P. Merkel, D.H. Miller, N. Neumeister, I. Shipsey, D. Silvers, A. Svyatkovskiy, M. Vidal Marono, H.D. Yoo, J. Zablocki, Y. Zheng

Purdue University Calumet, Hammond, USA

S. Guragain, N. Parashar

Rice University, Houston, USA

A. Adair, B. Akgun, C. Boulahouache, K.M. Ecklund, F.J.M. Geurts, W. Li, B.P. Padley, R. Redjimi, J. Roberts, J. Zabel

University of Rochester, Rochester, USA

B. Betchart, A. Bodek, Y.S. Chung, R. Covarelli, P. de Barbaro, R. Demina, Y. Eshaq, T. Ferbel, A. Garcia-Bellido, P. Goldenzweig, J. Han, A. Harel, D.C. Miner, D. Vishnevskiy, M. Zielinski

The Rockefeller University, New York, USA

A. Bhatti, R. Ciesielski, L. Demortier, K. Goulianos, G. Lungu, S. Malik, C. Mesropian

Rutgers, The State University of New Jersey, Piscataway, USA

S. Arora, A. Barker, J.P. Chou, C. Contreras-Campana, E. Contreras-Campana, D. Duggan, D. Ferencek, Y. Gershtein, R. Gray, E. Halkiadakis, D. Hidas, A. Lath, S. Panwalkar, M. Park, R. Patel, V. Rekovic, J. Robles, K. Rose, S. Salur, S. Schnetzer, C. Seitz, S. Somalwar, R. Stone, S. Thomas, M. Walker

University of Tennessee, Knoxville, USA

G. Cerizza, M. Hollingsworth, S. Spanier, Z.C. Yang, A. York

Texas A&M University, College Station, USA

R. Eusebi, W. Flanagan, J. Gilmore, T. Kamon[61], V. Khotilovich, R. Montalvo, I. Osipenkov, Y. Pakhotin, A. Perloff, J. Roe, A. Safonov, T. Sakuma, S. Sengupta, I. Suarez, A. Tatarinov, D. Toback

JHEP05(2013)090

Texas Tech University, Lubbock, USA

N. Akchurin, J. Damgov, C. Dragoiu, P.R. Dudero, C. Jeong, K. Kovitanggoon, S.W. Lee, T. Libeiro, I. Volobouev

Vanderbilt University, Nashville, USA

E. Appelt, A.G. Delannoy, C. Florez, S. Greene, A. Gurrola, W. Johns, P. Kurt, C. Maguire, A. Melo, M. Sharma, P. Sheldon, B. Snook, S. Tuo, J. Velkovska

University of Virginia, Charlottesville, USA

M.W. Arenton, M. Balazs, S. Boutle, B. Cox, B. Francis, J. Goodell, R. Hirosky, A. Ledovskoy, C. Lin, C. Neu, J. Wood

Wayne State University, Detroit, USA

S. Gollapinni, R. Harr, P.E. Karchin, C. Kottachchi Kankanamge Don, P. Lamichhane, A. Sakharov

University of Wisconsin, Madison, USA

M. Anderson, D.A. Belknap, L. Borrello, D. Carlsmith, M. Cepeda, S. Dasu, E. Friis, L. Gray, K.S. Grogg, M. Grothe, R. Hall-Wilton, M. Herndon, A. Hervé, P. Klabbers, J. Klukas, A. Lanaro, C. Lazaridis, R. Loveless, A. Mohapatra, M.U. Mozer, I. Ojalvo, F. Palmonari, G.A. Pierro, I. Ross, A. Savin, W.H. Smith, J. Swanson

†: Deceased
1: Also at Vienna University of Technology, Vienna, Austria
2: Also at CERN, European Organization for Nuclear Research, Geneva, Switzerland
3: Also at National Institute of Chemical Physics and Biophysics, Tallinn, Estonia
4: Also at California Institute of Technology, Pasadena, USA
5: Also at Laboratoire Leprince-Ringuet, Ecole Polytechnique, IN2P3-CNRS, Palaiseau, France
6: Also at Suez Canal University, Suez, Egypt
7: Also at Zewail City of Science and Technology, Zewail, Egypt
8: Also at Cairo University, Cairo, Egypt
9: Also at Fayoum University, El-Fayoum, Egypt
10: Also at British University in Egypt, Cairo, Egypt
11: Now at Ain Shams University, Cairo, Egypt
12: Also at National Centre for Nuclear Research, Swierk, Poland
13: Also at Université de Haute Alsace, Mulhouse, France
14: Also at Joint Institute for Nuclear Research, Dubna, Russia
15: Also at Skobeltsyn Institute of Nuclear Physics, Lomonosov Moscow State University, Moscow, Russia
16: Also at Brandenburg University of Technology, Cottbus, Germany
17: Also at The University of Kansas, Lawrence, USA
18: Also at Institute of Nuclear Research ATOMKI, Debrecen, Hungary
19: Also at Eötvös Loránd University, Budapest, Hungary
20: Also at Tata Institute of Fundamental Research - HECR, Mumbai, India
21: Now at King Abdulaziz University, Jeddah, Saudi Arabia
22: Also at University of Visva-Bharati, Santiniketan, India

JHEP05(2013)090

23: Also at Sharif University of Technology, Tehran, Iran
24: Also at Isfahan University of Technology, Isfahan, Iran
25: Also at Shiraz University, Shiraz, Iran
26: Also at Plasma Physics Research Center, Science and Research Branch, Islamic Azad University, Tehran, Iran
27: Also at Facoltà Ingegneria, Università di Roma, Roma, Italy
28: Also at Università degli Studi Guglielmo Marconi, Roma, Italy
29: Also at Università degli Studi di Siena, Siena, Italy
30: Also at University of Bucharest, Faculty of Physics, Bucuresti-Magurele, Romania
31: Also at Faculty of Physics, University of Belgrade, Belgrade, Serbia
32: Also at University of California, Los Angeles, USA
33: Also at Scuola Normale e Sezione dell'INFN, Pisa, Italy
34: Also at INFN Sezione di Roma, Roma, Italy
35: Also at University of Athens, Athens, Greece
36: Also at Rutherford Appleton Laboratory, Didcot, United Kingdom
37: Also at Paul Scherrer Institut, Villigen, Switzerland
38: Also at Institute for Theoretical and Experimental Physics, Moscow, Russia
39: Also at Albert Einstein Center for Fundamental Physics, Bern, Switzerland
40: Also at Gaziosmanpasa University, Tokat, Turkey
41: Also at Adiyaman University, Adiyaman, Turkey
42: Also at Izmir Institute of Technology, Izmir, Turkey
43: Also at The University of Iowa, Iowa City, USA
44: Also at Mersin University, Mersin, Turkey
45: Also at Ozyegin University, Istanbul, Turkey
46: Also at Kafkas University, Kars, Turkey
47: Also at Suleyman Demirel University, Isparta, Turkey
48: Also at Ege University, Izmir, Turkey
49: Also at Mimar Sinan University, Istanbul, Istanbul, Turkey
50: Also at Kahramanmaras Sütcü Imam University, Kahramanmaras, Turkey
51: Also at School of Physics and Astronomy, University of Southampton, Southampton, United Kingdom
52: Also at INFN Sezione di Perugia; Università di Perugia, Perugia, Italy
53: Also at Utah Valley University, Orem, USA
54: Now at University of Edinburgh, Scotland, Edinburgh, United Kingdom
55: Also at Institute for Nuclear Research, Moscow, Russia
56: Also at University of Belgrade, Faculty of Physics and Vinca Institute of Nuclear Sciences, Belgrade, Serbia
57: Also at Argonne National Laboratory, Argonne, USA
58: Also at Erzincan University, Erzincan, Turkey
59: Also at Yildiz Technical University, Istanbul, Turkey
60: Also at KFKI Research Institute for Particle and Nuclear Physics, Budapest, Hungary
61: Also at Kyungpook National University, Daegu, Korea

JHEP05(2013)090